

AD-A192 122

NEUTRON FIELD MEASUREMENTS IN PHANTOM WITH FOIL
ACTIVATION METHODS. (U) SCIENCE APPLICATIONS
INTERNATIONAL CORP SAN DIEGO CA V V VERBINSKI ET AL.

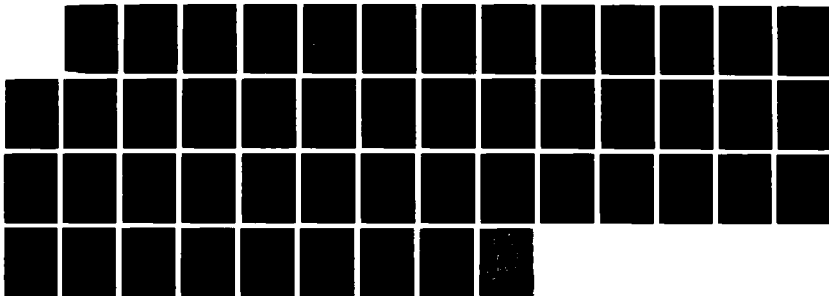
1/1

UNCLASSIFIED

29 NOV 86 SAIC-85-1898-R DMA-TR-87-10

F/G 24/6

ML



1-0

1-1

1-25

EEEEEE

1-4

2-8

3-15

3-5

4-0

4-5

1-2

2-2

2-0

1-8

1-6

AD-A192 122

FILE COPY

DNA-TR-87-10

4

NEUTRON FIELD MEASUREMENTS IN PHANTOM WITH FOIL ACTIVATION METHODS

V. V. Verbinski
C. G. Cassapakis
Science Applications International Corporation
10401 Roselle Street
San Diego, CA 92121

29 November 1986

Technical Report

CONTRACT No. DNA 001-83-C-0278

Approved for public release;
distribution is unlimited.

THIS WORK WAS SPONSORED BY THE DEFENSE NUCLEAR AGENCY
UNDER RDT&E RMSS CODE B350083466 U99QMXMK00062 H2590D.

DTIC
ELECTE
MAR 01 1988
S Ce H D

Prepared for
Director
DEFENSE NUCLEAR AGENCY
Washington, DC 20305-1000

88 2 29 10 5

Destroy this report when it is no longer needed. Do not return to sender.

PLEASE NOTIFY THE DEFENSE NUCLEAR AGENCY
ATTN: TITL, WASHINGTON, DC 20305 1000, IF YOUR
ADDRESS IS INCORRECT, IF YOU WISH IT DELETED
FROM THE DISTRIBUTION LIST, OR IF THE ADDRESSEE
IS NO LONGER EMPLOYED BY YOUR ORGANIZATION.



DISTRIBUTION LIST UPDATE

This mailer is provided to enable DNA to maintain current distribution lists for reports. We would appreciate your providing the requested information.

- ☐ Add the individual listed to your distribution list.
- ☐ Delete the cited organization/individual.
- ☐ Change of address.

NAME: _____

ORGANIZATION: _____

OLD ADDRESS

CURRENT ADDRESS

TELEPHONE NUMBER: () _____

SUBJECT AREA(s) OF INTEREST:

DNA OR OTHER GOVERNMENT CONTRACT NUMBER: _____

CERTIFICATION OF NEED-TO-KNOW BY GOVERNMENT SPONSOR (if other than DNA):

SPONSORING ORGANIZATION: _____

CONTRACTING OFFICER OR REPRESENTATIVE: _____

SIGNATURE: _____

CUT HERE AND RETURN



Director
Defense Nuclear Agency
ATTN: [REDACTED] TITL
Washington, DC 20305-1000

Director
Defense Nuclear Agency
ATTN: [REDACTED] TITL
Washington, DC 20305-1000

UNCLASSIFIED
SECURITY CLASSIFICATION OF THIS PAGE

AD-A192122

REPORT DOCUMENTATION PAGE				
1a. REPORT SECURITY CLASSIFICATION UNCLASSIFIED		1b. RESTRICTIVE MARKINGS		
2a. SECURITY CLASSIFICATION AUTHORITY N/A since Unclassified		3. DISTRIBUTION / AVAILABILITY OF REPORT Approval for public release; distribution is unlimited.		
2b. DECLASSIFICATION / DOWNGRADING SCHEDULE N/A since Unclassified				
4. PERFORMING ORGANIZATION REPORT NUMBER(S) SAIC-85-1090-R		5. MONITORING ORGANIZATION REPORT NUMBER(S) DNA-TR-87-10		
6a. NAME OF PERFORMING ORGANIZATION Science Applications International Corporation		6b. OFFICE SYMBOL (If applicable)	7a. NAME OF MONITORING ORGANIZATION Director Defense Nuclear Agency	
6c. ADDRESS (City, State, and ZIP Code) 10401 Roselle Street San Diego, CA 92121		7b. ADDRESS (City, State, and ZIP Code) Washington, DC 20305-1000		
8a. NAME OF FUNDING / SPONSORING ORGANIZATION		8b. OFFICE SYMBOL (If applicable) MR Col Harrison	9. PROCUREMENT INSTRUMENT IDENTIFICATION NUMBER DNA 001-83-C-0278	
8c. ADDRESS (City, State, and ZIP Code)		10. SOURCE OF FUNDING NUMBERS		
		PROGRAM ELEMENT NO 62715H	PROJECT NO U99QMXM	TASK NO X
				WORK UNIT ACCESSION NO DH006917
11. TITLE (Include Security Classification) NEUTRON FIELD MEASUREMENTS IN PHANTOM WITH FOIL ACTIVATION METHODS				
12. PERSONAL AUTHOR(S) Verbinski, Victor V.; Cassapakis, Costa G.				
13a. TYPE OF REPORT Technical		13b. TIME COVERED FROM 851129 TO 861129	14. DATE OF REPORT (Year, Month, Day) 861129	15. PAGE COUNT 46
16. SUPPLEMENTARY NOTATION This work was sponsored by the Defense Nuclear Agency under RDT&E RMSS Code B350083466 U99QMXMK00062 H2590D.				
17. COSATI CODES			18. SUBJECT TERMS (Continue on reverse if necessary and identify by block number)	
FIELD	GROUP	SUB-GROUP	Dosimetry; SAND II Neutron Measurements; Mid-Head Radiation Effects (Humans); ->Threshold Foil.	
6	7			
20	8			
19. ABSTRACT (Continue on reverse if necessary and identify by block number) <p>The threshold neutron-foil spectrometry method, utilizing the SAND II spectrum unfolding code, was evaluated by carrying out a measurement in the NBS standard fission source facility, simultaneous with six (6) in-phantom measurements of neutron spectra at the AFRRI Reactor Facility. The foil spectrometry was done with the full set of threshold foils, mid-thorax in ER1, where a 2nd lead wall separated reactor and phantom. A five-foil set was utilized for the phantom mid-head and phantom hip measurements in ER1, as well as for mid-thorax, mid-head and hip in ER2, free field. Calculations of the mid-thorax and mid-head spectra in ER1 and ER2 were carried out, with the source term normalized to nickel-foil activations at the reactor entrance window.</p> <p>A simple 5-foil perturbation method for neutron dosimetry, utilizing hand calculations, was developed and evaluated for the ER1 and ER2 spectra. It appears to be the order of 6 percent accurate versus 3-4 percent for SAND II, which utilizes the best (calculated) a priori data available for spectral shape information. <i>Keywords</i></p>				
20. DISTRIBUTION / AVAILABILITY OF ABSTRACT <input type="checkbox"/> UNCLASSIFIED/UNLIMITED <input checked="" type="checkbox"/> SAME AS RPT <input type="checkbox"/> DTIC USERS			21. ABSTRACT SECURITY CLASSIFICATION UNCLASSIFIED	
22a. NAME OF RESPONSIBLE INDIVIDUAL Sandra E. Young			22b. TELEPHONE (Include Area Code) (202) 325-7042	22c. OFFICE SYMBOL DNA/CSTI

DD FORM 1473, 84 MAR

83 APR edition may be used until exhausted
All other editions are obsolete

SECURITY CLASSIFICATION OF THIS PAGE
UNCLASSIFIED

UNCLASSIFIED

SECURITY CLASSIFICATION OF THIS PAGE

18. SUBJECT TERMS (Continued)

Phantom
NBS Standard Source
Mid-Thorax
Hip

UNCLASSIFIED

SECURITY CLASSIFICATION OF THIS PAGE

TABLE OF CONTENTS

SECTION	PAGE
List of Illustrations	iv
List of Tables	v
1 Introduction	1
2 Cross Calibration in NBS Standard Neutron Field	2
3 SAND II Measurements in Phantom	6
4 The 5-Foil Neutron Dosimetry Method	29
5 Comparison of SAND II and Simple 5-Foil Dosimetry Method	34
6 Thermal Neutron Dose	35
7 List of References	36



Accession For	
NTIS GRA&I	<input checked="" type="checkbox"/>
DTIC TAB	<input type="checkbox"/>
Unannounced	<input type="checkbox"/>
Justification	
By	
Distribution/	
Availability	
Dist	Spec
A-1	

LIST OF ILLUSTRATIONS

FIGURE	PAGE
1 ER1 Exposure Room Top View, Rhesus Monkey Phantom. ER2 is same but without Lead Wall.	3
2 View Perpendicular to Reactor-Phantom Center Line: ER1 and ER2 Exposure Room Configurations.	9
3 NBS Standard-Neutron-Field Measurement.	10
4 Orientation of Simple Phantom and Chair within the Plywood Enclosure.	11
5 ER1, Mid-Thorax, Max. Absolute Comparison of Calculation with Baseline Measurement.	17
6 ER1 Mid-Thorax. Min. Absolute Comparison.	18
7 ER1, Head, Absolute Data.	19
8 ER1-Hip, Measured, with Calculated Trail-Spectrum (Mid-Thorax) Fitted to it.	20
9 ER2, Mid Thorax, Absolute Fluences.	21
10 ER2, Head, Absolute Data.	22
11 ER2-Hip, Measured Spectrum with Trial Spectrum Normalized to it for Shape Comparison.	23
12 Spectrum-Shade Comparison, Mid Thorax: Effects of Lead Wall Shield (ER1).	24

LIST OF TABLES

TABLE	PAGE
1 NBS Cross-Calibration Run Activations Pertinent Parameters & Corrections	4
2 Basepoint Run (All Foils Present) Activations ER1: Mid-Thorax	7
3 Mini-Run (6 Foils Only) Activations Used for Unfolding	8
4 Comparison of Basepoint Run (All Foils Present) with Mini-Run (6 Foils Only) for ER1, Mid-Thorax Group Fluences, Doses	13
5 ER1 Calculated & Measured Group Fluences and Doses	14
6 ER2 Calculated & Measured Group Fluences and Doses at 100 cm from Reactor Dimple	15
7 Four-Group Comparison of Calculated Neutron Fluence and Dose with Baseline Measurements	28
8 Standard Run Parameters for Short-Stack Dosimetry at AFRRRI	31
9 Dose Determinations via 5-Foil Dosimetry Stack	32

SECTION 1 INTRODUCTION

The primary goal of this program was to provide a simplified, accurate method of neutron dosimetry for radiobiological studies, so that quantitative assessments of radiobiological effects would not be limited by the accuracy of the dose-measurement method (the cause), but rather by the less reproducible bio-effects (the effect). The probability that such a method will be put to use is a direct function of its accuracy and an inverse function of its costs in turnaround time, manpower, materials, and required expertise or sophistication. The method as presented in Section 4 below incorporates four neutron activation foils with natural thresholds extending from about 0.5 MeV to 8.7 MeV, plus cadmium-covered and bare gold foils (0.414×10^{-6} MeV and 0 MeV "thresholds"). It utilizes simple hand-processing of the data and is the order of 6% accurate.

Section 2 presents the "calibration" of the ASTM Standard threshold-foil spectrometry method¹⁻⁴ in the NBS Standard Neutron Field, to establish its accuracy. This method employs the SAND II unfolding code, and was used in AFRRRI monkey phantom measurements to provide a basis for evaluating the simple 5-foil (plus cadmium-covered gold) dosimetry method presented in Section 4.

Section 3 presents the results of this same type of spectrum/dose measurement, as carried out at several points inside the monkey phantom. The measurements were carried out both with the standard full dosimetry packet, the "full stack" (i.e., the baseline measurement), and with a much smaller, simplified packet, the "short stack." The accuracy of the short stack, as compared to the full stack, is demonstrated. In this section the dosimetry results, utilizing the SAND II spectrum unfolding code, are compared to the calculated data for absolute spectral flux/dose.

Section 4 presents the development of the simplified "short stack" method and assesses the accuracy of this straightforward, hand-calculational method of threshold-foil neutron dosimetry. The prescription for carrying out accurate dosimetry measurements with the simplified "short stack" method is also presented here.

SECTION 2

CROSS-CALIBRATION IN NBS STANDARD NEUTRON FIELD

A set of seven (7) neutron activation foils was irradiated in the NBS Standard Neutron Field in order to cross-calibrate the threshold foil method of neutron spectrometry. The foils were counted and the data were input to the SAND II unfolding code to obtain the neutron spectrum. A trial spectrum was also input to SAND II. This was the evaluated U-235 fission neutron spectrum discussed below (Figure 1).

Table 1 presents the neutron foil activations, as well as corrections in the NBS Standard Neutron Field for the flux activations gradient and for self-scattering by each foil.

Figure 1 shows the SAND II output spectrum as well as the evaluated U-235 fission neutron spectrum (Designation: XU5-5N1), corresponding to a fluence of $7.786 \times 10^{13} \text{ n/cm}^2$, $\pm 1.7\%$. The corresponding measured value utilizing the ASTM Standard methodology¹⁻⁴ yielded a fluence of $7.98 \times 10^{13} \text{ n/cm}^2$, which is within 2.5% of the NBS value: this is the first and only time the ASTM Method used here has been so evaluated.

Thus, the accuracy of the threshold-foil-spectrometry method, as carried out here, appears to be in the vicinity of 2-3% for a fission-type spectrum. For a water-cooled, water-moderated reactor spectrum, a 1/E tail exists below the fission-like spectrum. However, this 1/E shape is pretty much a canonical appendage; i.e., it is known to rather good accuracy. Therefore, the projected accuracy for a water-moderated reactor is probably the order of 3-4%, based on the NBS calibration results.

It should be pointed out that while the SAND II "calibration" produced a value of neutron fluence within 2.5% of the NBS standard, fluences obtained from some of the individual detectors showed variations approaching 10%. The strength of the multiple-foil approach is apparent here in that those foils departing furthest from the average, after folding in each one with the trial spectrum, are weighted the least. The final spectrum was obtained from the evaluated spectrum (used as input to SAND II) with only one very mild iteration. The spectral-shape constraint, as well as the de-emphasis by the

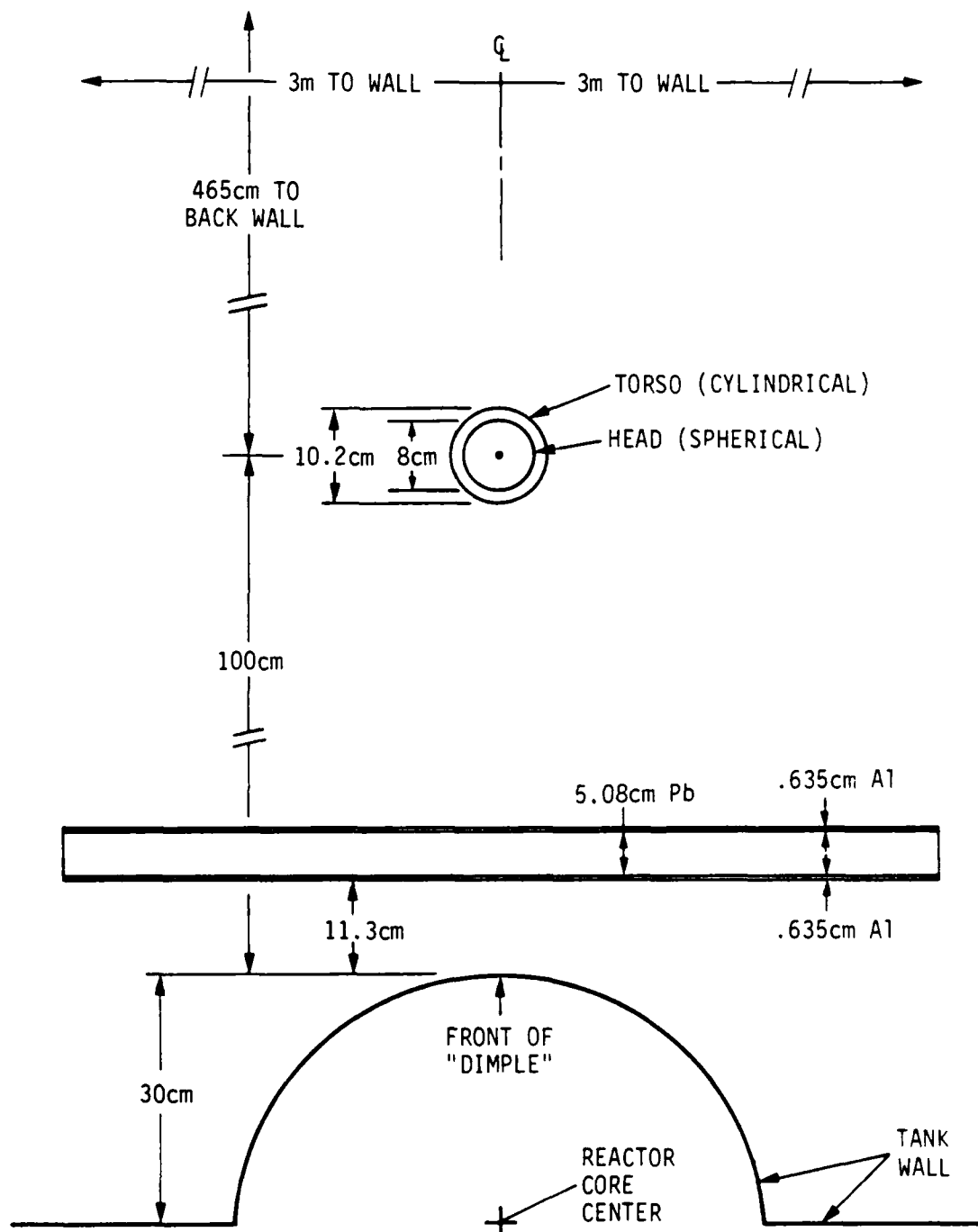


Figure 1. ER1 Exposure Room Top View, Rhesus Monkey Phantom.
ER2 is same but without Lead Wall.

Table 1. NBS Cross-Calibration Run Activations^a
Pertinent Parameters & Corrections.

Foil	$E_n^{th}(\text{MeV})$	$E_\gamma(\text{MeV})$	$\lambda(\text{hr}^{-1})$	V_T	V_f	$M_0\lambda(\text{un})^b$	f_{scat}	$f_{position}$	$M_0\lambda(\text{co})$
Rp-237	0.50	0.743 1.596	4.126-2 ^{cc} 1.723-2	0.92 0.96	0.0568 0.0548	1.02-10	0.972	1.049	1.04-10
In-115	1.00	0.335	1.540-1	0.50	---	5.09-16	1.000	1.079	6.36-16
W-238	1.45	0.537 0.743 1.596	2.256-3 4.126-2 1.723-2	0.256 0.92 0.96	0.0588 0.0509 0.0588	2.12-11	0.960	0.994	2.02-11
Fe-54	2.20	0.035	9.532-5	1.00	---	1.56-19	1.000	1.021	1.61-19
Mn-50	2.90	0.010	4.051-4	0.99	---	0.37-19	1.010	1.000	0.45-19
Mg-24	6.30	1.369	4.621-2	1.00	---	1.26-10	1.025	1.049	1.36-10
Al-27	0.70	1.369	4.621-2	1.00	---	6.13-19	1.021	1.042	6.52-19

^a M_0 and $M_0\lambda$ are given for the fission and non-fission foil activations, respectively

^{cc} Read as 4.126×10^{-2}

E_n^{th} - Neutron activation threshold energy

E_γ - Gamma ray energy

V_T - Fluorescent Yield

V_f - Fission Yield

$M_0\lambda(\text{un})$ - Foil activation (sec-1) uncorrected for scattering and position effects

f_{scat} - Foil scattering correction factor; accounts for deviation from neutron-free field due to the presence of the foil

f_{pos} - Foil position correction factor normalized to fluence at the M1 foil ($7.79 \pm 1.7\%$)

$M_0\lambda(\text{co})$ - Foil activation (sec-1) corrected for scattering and position effects

code of those foils that are in greatest disagreement in terms of the least-squares fit, result in a multi-foil accuracy considerably greater than that implied by the worst-foil variation. The numerous contributors to the errors in the NBS test include the following.

1. Uncertainty in NBS absolute field strength.
2. Uncertainty in the flux-gradient and self-absorption corrections.
3. Evaluated fission-spectrum-shape uncertainties.
4. Errors inherent in histogram-type approximation to the trial spectrum (the evaluated spectrum).
5. Threshold-foil cross section uncertainties.
6. Gamma-ray-line measurement uncertainties, including NBS-traceable calibration gamma-ray source uncertainties, fluorescent-yield uncertainties, fission branching ratio uncertainties (for fission foils), activation gamma-ray line decay time corrections, and counting statistics.

Efforts were made to reduce many of the uncertainties related to Item 6 above. A large improvement was achieved, as evidenced by the fact that all of the SAND II results, those for the NBS foils as well as those for all the AFRR1 phantom spectra presented below, required only one or two mild spectral-change perturbations; a large improvement over earlier measurements⁵ of the same kind.

In summary, an accuracy estimate of 3-4% for the AFRR1 monkey phantom measurements appears to be quite reasonable. The monkey phantom spectrum differs from the NBS U-235 fission spectrum in that the former has a 1/E tail plus thermal-neutron peak. However, the 1/E tail has a well-known and accurately calculable shape, and only contributes about 11% to the ER1, mid-thorax dose. The thermal peak is not part of this accuracy evaluation, as it can be handled both experimentally and calculationaly as an isolated case. (See Section 6 for details.)

SECTION 3

SAND II MEASUREMENTS IN PHANTOM

This section presents a series of six in-phantom spectrum measurements carried out with the short stack of dosimetry foils, one of which was also carried out with the full complement of foils. This will be referred to as the full-stack measurement or the basepoint measurement: It is the measurement which serves as a basepoint for the simplified 5-foil dosimetry method presented in Section 4. (See Tables 2 and 3 for the full-stack and the six short-stack foil data, respectively.)

The accuracy of the basepoint measurement was established in Section 2 above where all but the (unnecessary) low-energy neutron-sensitive foils were used for measuring a hard (unmoderated) fission spectrum. In this section, the accuracy of the short stack is evaluated by carrying out the SAND II unfolding both with the short stack and the full stack at the basepoint; i.e., at the mid-thorax point in ER1 (Exposure Room 1), where a 2"-thick lead gamma-ray shield was placed between the reactor and the phantom. (Since 0" to 6" of lead shielding has been used for in-phantom dosimetry measurements, the ER1 exposure turned out to be a good choice for the basepoint measurement. This is especially important for the simplified, hand-calculated dosimetry method developed here and presented in Section 4 below because the 2" lead wall neutron spectrum is intermediate in "softness" between the 0" and 6" lead-shield neutron spectra.)

Figure 2 shows the experimental configuration for the ER1 area, where a 2"-thick lead-wall gamma-ray shield was used. The ER2 configuration was identical, except that no lead shield was used there, and the center of the phantom was 100 cm from the front of the reactor dimple in ER2, instead of 130 cm.

Figure 3 shows a cutaway view, through the rhesus monkey phantom and perpendicular to the reactor-phantom center line, and Figure 4 shows the simple phantom and chair within the plywood enclosure.

Table 2. Basepoint Run (All Foils Present) Activations
ER1: Mid-Thorax.

Foil*	E_n^{th} (MeV)	E_γ (MeV)	λ (hr ⁻¹)	γ_γ	γ_f	$N_0 \lambda$ (sec ⁻¹)**
¹⁹⁷ Au	0 ⁺	0.412	1.071-2 ⁺⁺	0.95	---	6.15-16
⁵⁵ Mn	0 ⁺	0.847	2.687-1	0.99		3.66-16
		1.811	2.687-1	0.29		
²³⁵ U	0 ⁺	0.537	2.256-3	0.26	0.0626	8.93-11
		0.743	4.126-2	0.92	0.0648	
		1.596	1.723-2	0.96	0.0626	
²³⁷ Np	0.50	0.743	4.236-2	0.92	0.0568	4.11-12
		1.596	1.723-2	0.96	0.0548	
¹¹⁵ In	1.00	0.335	1.540-1	0.50	---	2.25-17
²³⁸ U	1.45	0.537	2.256-3	0.256	0.0588	7.62-13
		0.743	4.126-2	0.92	0.0509	
		1.596	1.723-2	0.96	0.0588	
²³² Th	1.75	0.537	2.256-3	0.256	0.0760	1.78-13
		0.743	4.126-2	0.92	0.0534	
⁵⁴ Fe	2.20	0.835	9.532-5	1.00	---	5.87-21
⁵⁸ Ni	2.90	0.810	4.051-4	0.99	---	3.20-20
²⁴ Mg	6.30	1.369	4.621-2	1.00	---	6.08-20
²⁷ Al	8.70	1.369	4.621-2	1.00	---	3.02-20
⁹⁰ Zr	14.00	0.910	8.841-3	0.99	---	2.04-21

* All foils in 0.020" cadmium

** $N_0 \lambda$ in sec⁻¹ is given for the non-fission foils only
 N_0 is given for the fission foils

+ Since the foils are enclosed in cadmium, the effective threshold for these foils is actually 4.25-7 MeV

++ Read as 1.071×10^{-2}

Table 3. Mini-Run (6 Foils Only) Activations
Used for Unfolding.

<u>Foil</u> [*]	$N_0 \lambda \text{ (sec}^{-1}\text{): ER1}$			$N_0 \lambda \text{ (sec}^{-1}\text{): ER2}$		
	<u>Thorax</u> ^{**}	<u>Head</u>	<u>Hip</u>	<u>Thorax</u>	<u>Head</u>	<u>Hip</u>
¹⁹⁷ Au ⁺	6.15-16 ⁺⁺	5.65-16	6.98-16	1.51-15	1.32-15	1.78-15
¹¹⁵ In	2.25-17	2.10-17	2.86-17	6.59-17	5.57-17	7.68-17
⁵⁴ Fe	5.87-21	5.71-21	7.27-21	1.97-20	1.60-20	2.08-20
⁵⁸ Ni	3.20-20	3.03-20	3.81-20	1.08-19	8.81-20	1.19-19
²⁴ Mg	6.08-20	5.82-20	6.81-20	2.21-19	1.75-19	2.43-19
²⁷ Al	3.02-20	3.07-20	3.52-20	1.08-19	8.99-20	1.15-19

* All foils in .020" cadmium cover

** These activations are taken from the standard (all foils present) run

+ For a complete list of activation parameters, cf, either Table 1 or 2

++ Read as 6.15×10^{-16}

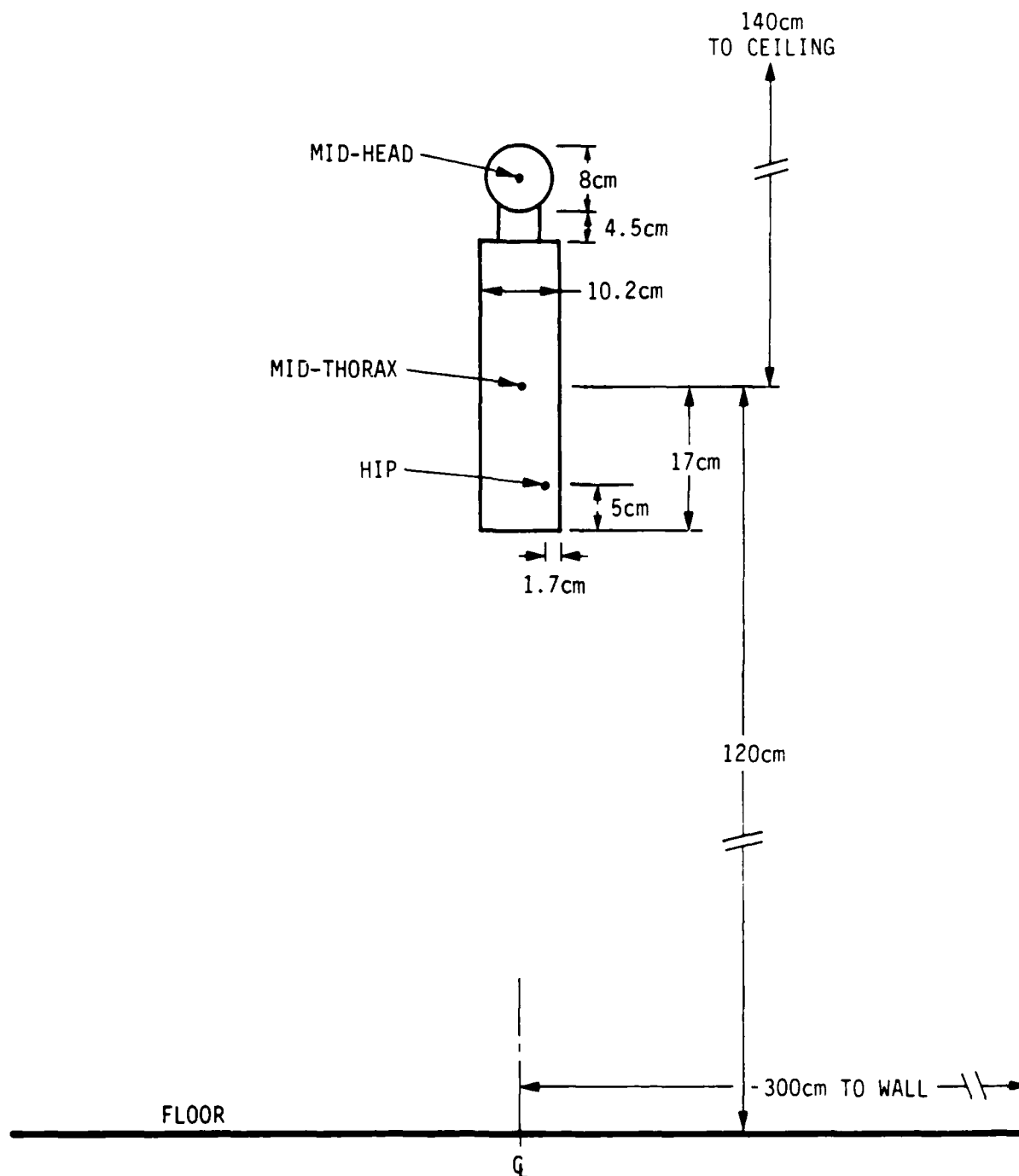


Figure 2. View Perpendicular to Reactor-Phantom Center Line: ER1 and ER2 Exposure Room Configurations.

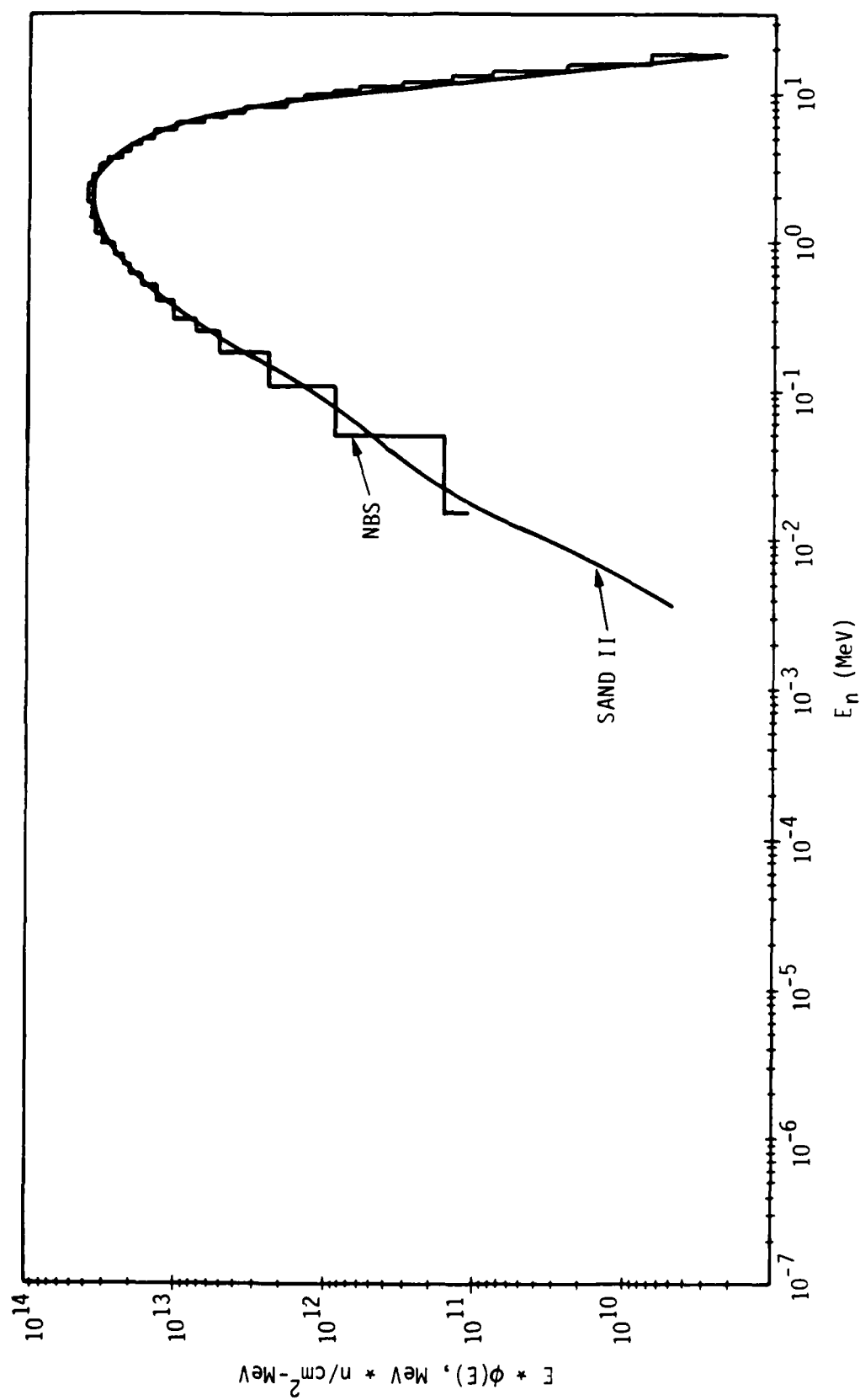


Figure 3. NBS Standard-Neutron-Field Measurement.

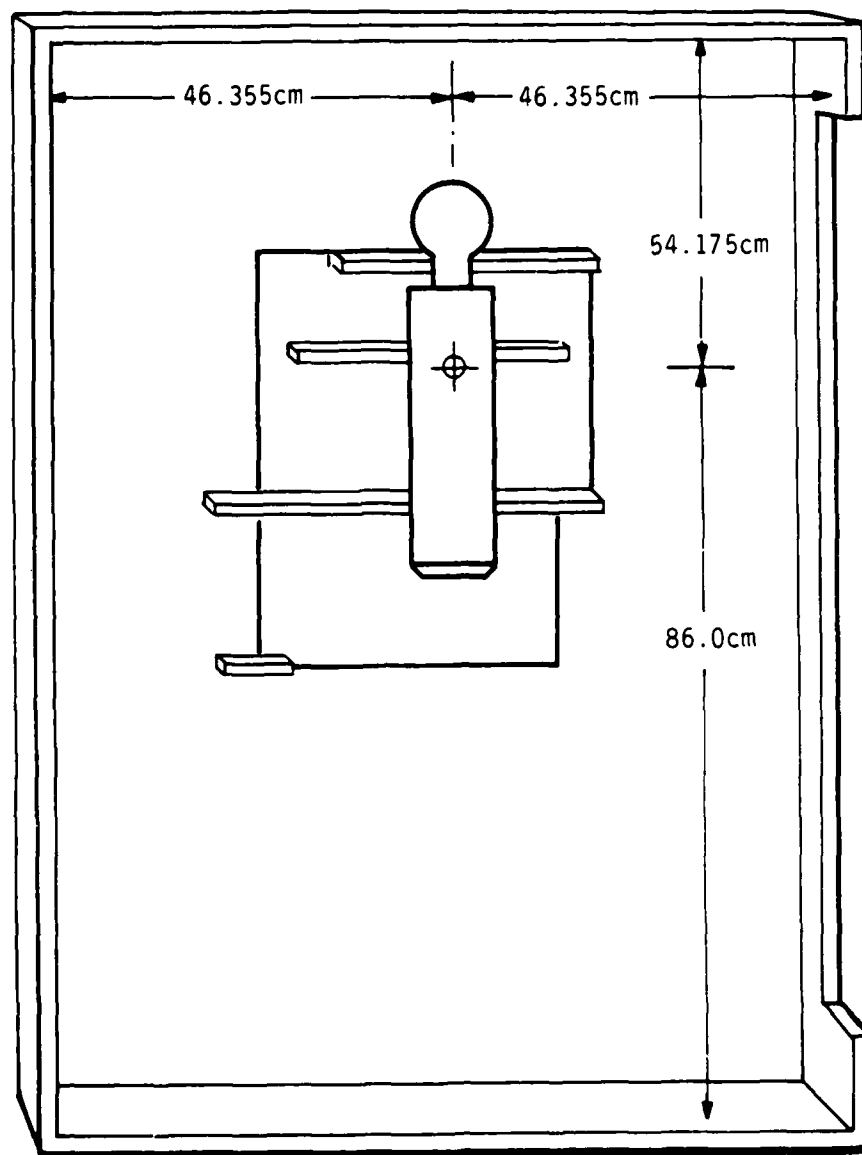


Figure 4. Orientation of Simple Phantom and Chair within the Plywood Enclosure.

The threshold-foil activation data for the full stack of dosimetry foils, the full complement of (ASTM Standard) neutron activation foils, is presented in Table 2 for the rhesus monkey phantom mid-thorax spectrometry/dosimetry exposure in ER1, behind the 2" lead shield; i.e., the basepoint measurement. The threshold-foil data for the six (6) short stack exposures are presented in Table 3, with the ER1 mid-thorax data being common to the Table 2 data. All foils presented in Tables 2 and 3 were cadmium-covered, with a watertight 0.020"-thick cadmium enclosure. The bare gold and manganese foils were exposed in a separate but otherwise identical reactor run, and the activations are not presented in the interest of brevity.

The thermal group is group 37, and the fluence/dose determination is achieved with a simple hand calculation utilizing the gold- or manganese-foil cadmium-difference activations: the methodology of Sections 3 and 4 does not apply to the thermal-neutron fluence/dose. This is adequately covered in Section 6, in terms of the goals of this work.

Table 4 presents a comparison of the SAND II spectrum unfolding code output for the basepoint measurement as carried out with the full stack (standard) and the short stack (labeled "mini"). The calculated spectrum/dose data are also presented in Tables 4, 5 and 6 for calculations carried out in the basepoint location (ER1, mid-thorax), at center head in ER1, and for both mid-thorax and center-head locations in ER2. The comparison of measured and calculated data is presented in Section 3.2 below and includes the experimental normalization of the calculational data, a vital point when considering that one would otherwise have to rely on chamber dosimeters, whose accuracy is, in effect, being evaluated by these more sophisticated spectrometry/dosimetry methods presented here.

The data of Table 4 show an agreement of 2% in total fluence between the full-stack and the short-stack SAND II code outputs. The doses agree to within about 1%. Application of a quicker, analytical technique utilizing these same threshold-foil activation data and the accuracy of that method are presented in Section 4 below. That accuracy assessment is, of course, based directly on the use of the SAND II results (Tables 4, 5 and 6), and on the adequacy of these baseline data.

Table 4. Comparison of Basepoint Run (All Foils Present) with Mini-Run (6 Foils Only) for ER1, Mid-Thorax - Group Fluences ($n/cm^2 \cdot kW \cdot Min$), Doses (Rad Tissue).

Group #	Upper Energy (MeV)	Calculated		Basepoint		Mini	
		ϕ_{Calc}	D_{Calc}	ϕ_{Meas}	D_{Meas}	ϕ_{Meas}	D_{Meas}
1	19.6	6.64+3	4.89-5	7.42+3	5.46-5	3.70+3	2.72-5
2	16.9	3.60+4	2.49-4	5.21+4	3.62-4	2.64+4	1.83-4
3	14.9	3.10+4	2.07-4	4.19+4	2.80-4	2.15+4	1.44-4
4	14.2	1.98+4	1.30-4	2.95+4	1.94-4	1.53+4	1.00-4
5	13.8	1.42+5	9.02-4	1.73+5	1.10-3	9.35+4	5.95-4
6	12.8	1.30+5	7.95-4	1.55+5	9.49-4	9.66+4	5.91-4
7	12.2	4.99+5	3.03-3	3.52+5	2.14-3	3.47+5	2.11-3
8	11.1	8.55+5	4.90-3	6.45+5	3.70-3	6.43+5	3.69-3
9	10.0	1.51+6	8.35-3	1.10+6	6.06-3	1.09+6	6.01-3
10	9.05	2.37+6	1.25-2	1.79+6	9.43-3	1.78+6	9.37-3
11	8.19	4.37+6	2.24-2	3.23+6	1.65-2	3.20+6	1.64-2
12	7.41	1.23+7	6.08-2	9.05+6	4.48-2	8.99+6	4.45-2
13	6.38	3.32+7	1.53-1	2.69+7	1.24-1	2.74+7	1.26-1
14	4.97	8.02+6	3.51-2	6.89+6	3.02-2	7.07+6	3.09-2
15	4.72	2.86+7	1.23-1	2.35+7	1.01-1	2.41+7	1.04-1
16	4.07	6.75+7	2.75-1	5.87+7	2.39-1	6.07+7	2.47-1
17	3.01	7.74+7	2.66-1	6.39+7	2.20-1	6.64+7	2.28-1
18	2.39	1.34+7	4.22-2	1.10+7	3.47-2	1.14+7	3.60-2
19	2.31	8.19+7	2.54-1	7.03+7	2.19-1	7.38+7	2.29-1
20	1.83	2.02+8	5.41-1	1.61+8	4.31-1	1.66+8	4.46-1
21	1.11	2.30+8	4.70-1	1.90+8	3.90-1	1.90+8	3.89-1
22	.550	1.97+8	2.51-1	1.71+8	2.17-1	1.61+8	2.04-1
23	.158	4.57+7	3.57-2	3.60+7	2.81-2	3.13+7	2.44-2
24	.111	9.51+7	5.17-2	7.16+7	3.90-2	6.31+7	3.43-2
25	.0525	8.11+7	2.49-2	6.04+7	1.85-2	5.32+7	1.63-2
26	.0248	1.05+7	2.18-3	8.23+6	1.72-3	7.22+6	1.51-3
27	.0219	7.93+7	1.14-2	5.60+7	8.01-3	4.96+7	7.11-3
28	.0103	9.04+7	5.52-3	6.93+7	4.23-3	6.22+7	3.80-3
29	3.35-3	8.49+7	1.83-3	6.49+7	1.40-3	5.85+7	1.26-3
30	1.23-3	8.50+7	7.66-4	6.04+7	5.45-4	5.41+7	4.88-4
31	5.83-4	1.72+8	5.36-4	1.24+8	3.87-4	1.10+8	3.43-4
32	1.01-4	1.20+8	1.46-4	8.52+7	1.03-4	7.75+7	9.40-5
33	2.40-5	9.66+7	1.22-4	7.24+7	9.12-5	6.49+7	8.20-5
34	1.07-6	1.51+8	2.96-4	9.91+7	1.94-4	9.12+7	1.78-4
35	3.06-6	8.83+7	2.93-4	6.88+7	2.28-4	6.08+7	2.02-4
36	1.13-6	9.59+7	5.22-4	5.76+7	3.13-4	5.10+7	2.78-4
37	4.14-7	4.34+9	9.72-2	2.84+9	6.37-2	2.84+9	6.37-2
Total		6.60+9	2.76+0	4.57+9	2.25+0	4.48+9	2.28+0

Table 5. ERI Calculated & Measured Group
Fluences ($n/cm^2 \cdot kW \cdot Min$) and Doses ($R/kW \cdot Min$).

Group θ	$E_0 (MeV)$	Mid-Thorax				Head				Hip			
		Φ_{Calc}	Φ_{Meas}	D_{Calc}	D_{Meas}	Φ_{Calc}	Φ_{Meas}	D_{Calc}	D_{Meas}	Φ_{Calc}	Φ_{Meas}	D_{Calc}	D_{Meas}
1	19.6	6.64+3	3.70+3	4.89-5	2.72-5	7.97+3	3.89+3	5.87-5	2.86-5	4.25+3	3.13-5	5.87-5	3.13-5
2	16.9	3.60+4	2.64+4	2.49-4	1.83-4	3.71+4	2.58+4	2.58-4	1.79-4	3.03+4	2.10-4	2.58-4	2.10-4
3	14.9	3.10+4	2.15+4	2.07-4	1.44-4	3.39+4	2.08+4	2.27-4	1.40-4	2.47+4	1.65-4	2.27-4	1.65-4
4	14.2	1.98+4	1.53+4	1.30-4	1.00-4	1.80+4	1.30+4	1.18-4	0.53-5	1.76+4	1.15-4	1.18-4	1.15-4
5	13.8	1.42+5	9.35+4	9.02-4	5.95-4	1.35+5	8.02+4	8.61-4	5.11-4	1.07+5	6.82-4	8.61-4	6.82-4
6	12.8	1.30+5	9.86+4	7.95-4	5.91-4	1.12+5	7.86+4	6.83-4	4.81-4	1.11+5	6.79-4	6.83-4	6.79-4
7	12.2	4.99+5	3.47+5	3.03-3	2.11-3	5.04+5	3.19+5	3.06-3	1.94-3	4.00+5	2.43-3	3.06-3	2.43-3
8	11.1	8.55+5	6.43+5	4.90-3	3.69-3	8.75+5	6.10+5	5.02-3	3.50-3	7.40+5	4.25-3	5.02-3	4.25-3
9	10.0	1.51+6	1.09+6	8.35-3	6.01-3	1.59+6	1.08+6	8.75-3	5.96-3	1.26+6	6.94-3	8.75-3	6.94-3
10	9.05	2.37+6	1.78+6	1.25-2	9.37-3	2.90+6	1.93+6	1.53-2	1.03-2	2.04+6	1.88-2	1.53-2	1.03-2
11	8.19	4.37+6	3.20+6	2.24-2	1.64-2	4.93+6	3.34+6	2.52-2	1.71-2	3.70+6	1.89-2	2.52-2	1.71-2
12	7.41	1.23+7	8.99+6	6.08-2	4.45-2	1.27+7	8.71+6	6.28-2	4.31-2	1.05+7	5.20-2	6.28-2	4.31-2
13	6.38	3.32+7	2.74+7	1.53-1	1.26-1	3.14+7	2.55+7	1.45-1	1.18-1	3.32+7	1.53-1	1.45-1	1.18-1
14	4.97	8.02+6	7.07+6	3.51-2	3.09-2	7.76+6	6.59+6	3.40-2	2.88-2	8.61+6	3.77-2	3.40-2	2.88-2
15	4.72	2.86+7	2.41+7	1.23-1	1.04-1	2.76+7	2.32+7	1.19-1	2.17-1	2.93+7	1.26-1	1.19-1	2.17-1
16	4.07	6.75+7	6.07+7	2.75-1	2.47-1	5.79+7	5.32+7	2.36-1	9.60-2	7.39+7	3.01-1	2.36-1	9.60-2
17	3.01	7.74+7	6.64+7	2.66-1	2.28-1	8.69+7	6.78+7	2.99-1	2.33-1	8.08+7	2.78-1	2.99-1	2.33-1
18	2.39	1.34+7	1.14+7	4.22-2	3.60-2	1.40+7	1.15+7	4.41-2	3.63-2	1.39+7	4.38-2	4.41-2	3.63-2
19	2.11	8.19+7	7.38+7	2.54-1	2.29-1	9.06+7	7.48+7	2.92-1	2.32-1	9.02+7	2.81-1	2.92-1	2.32-1
20	1.23	2.02+8	1.66+8	5.41-1	4.46-1	1.83+8	1.48+8	4.90-1	3.97-1	2.03+8	5.44-1	4.90-1	3.97-1
21	1.11	2.30+8	1.90+8	4.70-1	3.89-1	2.40+8	1.82+8	4.91-1	3.72-1	2.33+8	4.78-1	4.91-1	3.72-1
22	.55	1.97+8	1.61+8	2.51-1	2.04-1	2.30+8	1.88+8	2.92-1	2.39-1	1.91+8	2.43-1	2.92-1	2.39-1
23	.158	4.57+7	3.13+7	3.57-2	2.44-2	5.53+7	4.13+7	4.32-2	3.22-2	3.58+7	2.79-2	4.32-2	3.22-2
24	.111	9.51+7	6.31+7	5.17-2	3.43-2	7.86+7	6.35+7	4.27-2	3.45-2	7.16+7	3.90-2	4.27-2	3.45-2
25	.0525	8.11+7	5.32+7	2.49-2	1.63-2	7.61+7	5.77+7	2.33-2	1.77-2	6.04+7	1.85-2	2.33-2	1.77-2
26	.0248	1.05+7	7.22+6	2.18-3	1.51-3	1.25+7	9.74+6	2.61-3	2.03-3	8.22+6	1.72-3	2.61-3	2.03-3
27	.0219	7.93+7	4.96+7	1.14-2	7.11-3	6.53+7	2.75+7	9.37-3	3.94-3	5.65+7	8.08-3	9.37-3	3.94-3
28	.0103	9.04+7	6.22+7	5.52-3	3.80-3	1.12+8	1.04+8	6.86-3	6.35-3	7.07+7	4.32-3	6.86-3	6.35-3
29	3.35-3	5.85+7	5.05+7	1.83-3	1.26-3	9.53+7	7.30+7	2.06-3	1.57-3	6.63+7	1.43-3	2.06-3	1.57-3
30	1.23-3	8.50+7	5.41+7	7.66-4	4.88-4	8.45+7	6.10+7	7.62-4	5.50-4	6.16+7	5.56-4	7.62-4	5.50-4
31	5.83-4	1.72+8	1.10+8	5.36-4	3.43-4	1.70+8	1.23+8	5.29-4	3.84-4	1.25+8	3.90-4	5.29-4	3.84-4
32	1.01-4	1.20+8	7.75+7	1.46-4	9.40-5	1.26+8	9.07+7	1.53-4	1.10-4	8.80+7	1.06-4	1.53-4	1.10-4
33	2.40-5	9.66+7	6.49+7	1.22-4	8.20-5	1.00+8	7.31+7	1.27-4	9.24-5	4.69+7	5.91-5	1.27-4	9.24-5
34	1.07-5	1.51+8	9.12+7	2.96-4	1.78-4	1.14+8	8.50+7	2.24-4	1.66-4	1.31+8	2.57-4	2.24-4	1.66-4
35	3.06-6	8.83+7	6.08+7	2.93-4	2.02-4	9.78+7	7.26+7	3.25-4	2.41-4	6.90+7	2.29-4	3.25-4	2.41-4
36	1.13-6	9.59+7	5.10+7	5.22-4	2.78-4	1.10+8	6.50+7	5.96-4	3.54-4	5.81+7	3.16-4	5.96-4	3.54-4
37	4.14-7	4.34+9	2.84+9	9.72-2	6.37-2	3.32+9	2.98+9	7.44-2	6.62-2	3.70+9	8.28-2	7.44-2	6.62-2

Table 6. ER2 Calculated & Measured Group Fluences (n/cm² · kW · Min) and Doses (R/tW · Min) at 100 cm from Reactor Dimple.

Group	θ	E _g (MeV)	Mid-Thorax				Head				Hip			
			Φ _{Calc}	Φ _{Meas}	D _{Calc}	D _{Meas}	Φ _{Calc}	Φ _{Meas}	D _{Calc}	D _{Meas}	Φ _{Calc}	Φ _{Meas}	D _{Calc}	D _{Meas}
1		19.6	2.23+4	1.30+4	1.60-4	9.57-5	2.70+4	1.13+4	1.99-4	8.32-5	1.41+4	1.04-4	1.99-4	1.04-4
2		16.9	1.24+5	9.40+4	8.60-4	6.52-4	1.27+5	7.56+4	8.80-4	5.24-4	1.02+5	7.08-4	8.80-4	7.08-4
3		14.9	1.08+5	7.68+4	7.19-4	5.13-4	1.19+5	6.21+4	7.92-4	4.15-4	8.29+4	5.54-4	7.92-4	5.54-4
4		14.2	6.81+4	5.45+4	4.47-4	3.58-4	6.10+4	3.80+4	4.01-4	2.49-4	5.87+4	3.85-4	4.01-4	3.85-4
5		13.8	4.97+5	3.35+5	3.16-3	2.16-3	4.68+5	2.36+5	2.97-3	1.50-3	3.66+5	2.33-3	2.97-3	2.33-3
6		12.8	4.59+5	3.45+5	2.81-3	2.11-3	3.87+5	2.33+5	2.37-3	1.43-3	3.60+5	2.33-3	2.37-3	2.33-3
7		12.2	1.75+6	1.27+6	1.06-2	7.71-3	1.77+6	9.51+5	1.07-2	5.78-3	1.36+6	8.26-3	1.07-2	8.26-3
8		11.1	2.96+6	2.30+6	1.70-2	1.32-2	3.03+6	1.81+6	1.74-2	1.04-2	2.48+6	1.42-2	1.74-2	1.42-2
9		10.0	5.20+6	3.89+6	2.87-2	2.14-2	5.44+6	3.19+6	3.00-2	1.76-2	4.19+6	2.31-2	3.00-2	2.31-2
10		9.05	8.23+6	6.37+6	4.34-2	3.35-2	1.01+7	5.81+6	5.30-2	3.06-2	6.89+6	3.63-2	5.30-2	3.63-2
11		8.19	1.52+7	1.15+7	7.77-2	5.88-2	1.72+7	1.00+7	8.78-2	5.11-2	1.25+7	6.39-2	8.78-2	6.39-2
12		7.41	4.31+7	3.22+7	2.13-1	1.59-1	4.43+7	2.62+7	2.19-1	1.30-1	3.50+7	1.73-1	2.19-1	1.73-1
13		6.38	1.15+8	9.56+7	5.30-1	4.41-1	1.06+8	7.56+7	4.91-1	3.49-1	1.04+8	4.80-1	4.91-1	4.80-1
14		4.97	2.89+7	2.51+7	1.26-1	1.10-1	2.64+7	1.97+7	1.50-1	8.82-2	2.75+7	1.20-1	1.50-1	8.82-2
15		4.72	1.03+8	8.60+7	4.44-1	3.70-1	9.98+7	6.90+7	4.30-1	2.97-1	9.41+7	4.06-1	4.30-1	4.06-1
16		4.07	2.24+8	2.00+8	9.11-1	8.14-1	1.83+8	1.50+8	7.47-1	6.11-1	2.22+8	9.04-1	7.47-1	9.04-1
17		3.01	2.37+8	2.01+8	8.17-1	6.92-1	2.57+8	1.80+8	8.80-1	6.19-1	2.26+8	7.77-1	8.80-1	7.77-1
18		2.39	3.81+7	3.23+7	1.20-1	1.02-1	4.04+7	2.93+7	1.27-1	9.24-2	3.65+7	1.15-1	1.27-1	1.15-1
19		2.31	2.09+8	1.91+8	6.50-1	5.94-1	2.30+8	1.76+8	7.14-1	5.47-1	2.18+8	6.78-1	7.14-1	6.78-1
20		1.93	4.96+8	4.05+8	1.33+0	1.09+0	4.22+8	3.16+8	1.13+0	8.48-1	4.67+8	1.25+0	1.13+0	8.48-1
21		1.11	5.30+8	4.35+8	1.08+0	8.90-1	4.93+8	3.52+8	1.01+0	7.20-1	5.07+8	1.04+0	1.01+0	7.20-1
22		.55	4.17+8	3.59+8	5.30-1	4.56-1	4.46+8	3.77+8	5.66-1	4.79-1	4.22+8	5.36-1	5.66-1	4.79-1
23		.158	9.74+7	7.30+7	7.60-2	5.70-2	1.12+8	9.13+7	8.71-2	7.17-2	8.72+7	6.80-2	8.71-2	7.17-2
24		.111	2.00+8	1.47+8	1.09-1	7.99-2	1.57+8	1.41+8	8.51-2	7.67-2	1.74+8	9.47-2	8.51-2	7.67-2
25		.0525	1.89+8	1.28+8	5.78-2	3.92-2	1.66+8	1.34+8	5.08-2	4.11-2	1.52+8	4.67-2	5.08-2	4.11-2
26		.0248	2.07+7	1.60+7	4.32-3	3.34-3	2.54+7	2.16+7	5.30-3	4.51-3	1.78+7	3.72-3	5.30-3	4.51-3
27		.0219	1.72+8	1.14+8	2.47-2	1.63-2	1.39+8	1.19+8	1.99-2	1.71-2	1.36+8	1.94-2	1.99-2	1.71-2
28		.0103	1.88+8	1.42+8	1.15-2	8.67-3	2.30+8	1.82+8	1.40-2	1.11-2	1.71+8	1.04-2	1.40-2	1.11-2
29		3.35-3	1.82+8	1.38+8	3.92-3	2.98-3	1.94+8	1.63+8	4.19-3	3.51-3	1.61+8	3.48-3	4.19-3	3.51-3
30		1.21-3	1.85+8	1.28+8	1.67-3	1.15-3	1.65+8	1.31+8	1.49-3	1.16-3	1.52+8	1.37-3	1.49-3	1.16-3
31		5.83-4	3.56+8	2.52+8	1.11-3	7.86-4	3.36+8	2.68+8	1.05-3	8.36-4	2.99+8	9.33-4	1.05-3	8.36-4
32		1.01-4	2.63+8	1.83+8	3.19-4	2.22-4	2.61+8	2.04+8	3.17-4	2.47-4	2.16+8	2.64-4	3.17-4	2.47-4
33		2.40-5	2.04+8	1.52+8	2.58-4	1.92-4	1.96+8	1.58+8	2.48-4	2.00-4	1.79+8	2.26-4	2.48-4	2.00-4
34		1.07-5	3.41+8	2.20+8	6.67-4	4.31-4	2.47+8	1.98+8	4.74-4	3.87-4	2.63+8	5.15-4	4.74-4	3.87-4
35		3.06-6	1.90+8	1.46+8	6.32-4	4.85-4	2.10+8	1.71+8	6.97-4	5.68-4	1.71+8	5.68-4	6.97-4	5.68-4
36		1.13-6	2.14+8	1.23+8	1.16-3	6.70-4	2.38+8	1.54+8	1.30-3	8.38-4	1.47+8	8.00-4	1.30-3	8.38-4
37*		4.14-7	1.23+10	1.20+10	2.75-1	2.68-1	9.95+9	8.86+9	2.23-1	1.98-1	9.94+9	2.23-1	2.23-1	1.98-1

* The measured fluences and doses for the thermal group were determined from the bare and cadmium-covered Au foils activations. SAND II unfolding was not used for this group.

3.1 SPECTRAL SHAPES .

The SAND II unfolding results of the baseline measurements at the basepoint (ER1, mid-thorax) are shown for the standard dosimetry foil pack in Figure 5 and for the short stack in Figure 6. They are compared to the direct calculational outputs: these calculational data were normalized to some tissue-equivalent (TE) dosimetry measurements taken at some other (distant) time, and the agreement/disagreement with the absolute measurement is therefore misleading. A valid renormalization of the calculated data was done utilizing nickel foils placed on the front of the reactor dimple (see Figure 2), and a discussion of calculational predictions in magnitude is deferred to Section 3.2. The full-stack and short-stack data are in excellent agreement with one another in shape as well as magnitude. The agreement in shape with the calculated (trial) spectrum is also excellent, as evidenced by the fact that the SAND II code carried out its very minimum of only one iteration to obtain the final (measured) spectrum that is in accord with the threshold-foil data.

Figure 7 compares the absolute measured data with the calculated data, as normalized to some TE dosimeter measurement carried out at a different time. The agreement in spectral shape is indeed very good, as it is for the measurement in the rhesus monkey phantom hip in ER1. These data for the hip location, shown in Figure 8, utilized the neutron spectrum calculated at mid-thorax in ER1. The calculated spectrum was arbitrarily fitted to the absolute spectral flux measurement, in Figure 8, to show a good shape comparison.

Figures 9, 10 and 11 show in-phantom spectral data similar to that of Figures 6, 7 and 8, respectively, but for the free-field case (i.e., no lead shield) in ER2. Again, the measured spectral shapes are in good agreement with the calculated shapes.

In Figure 12, a comparison in spectral shape is shown between ER1 and ER2 spectra, mid-thorax. Note that the spectral shapes are practically identical below about 0.4 MeV. This is the "canonical slowing-down spectrum." As normalized in the slowing-down region, the ER1 spectrum above 0.4 MeV is seen

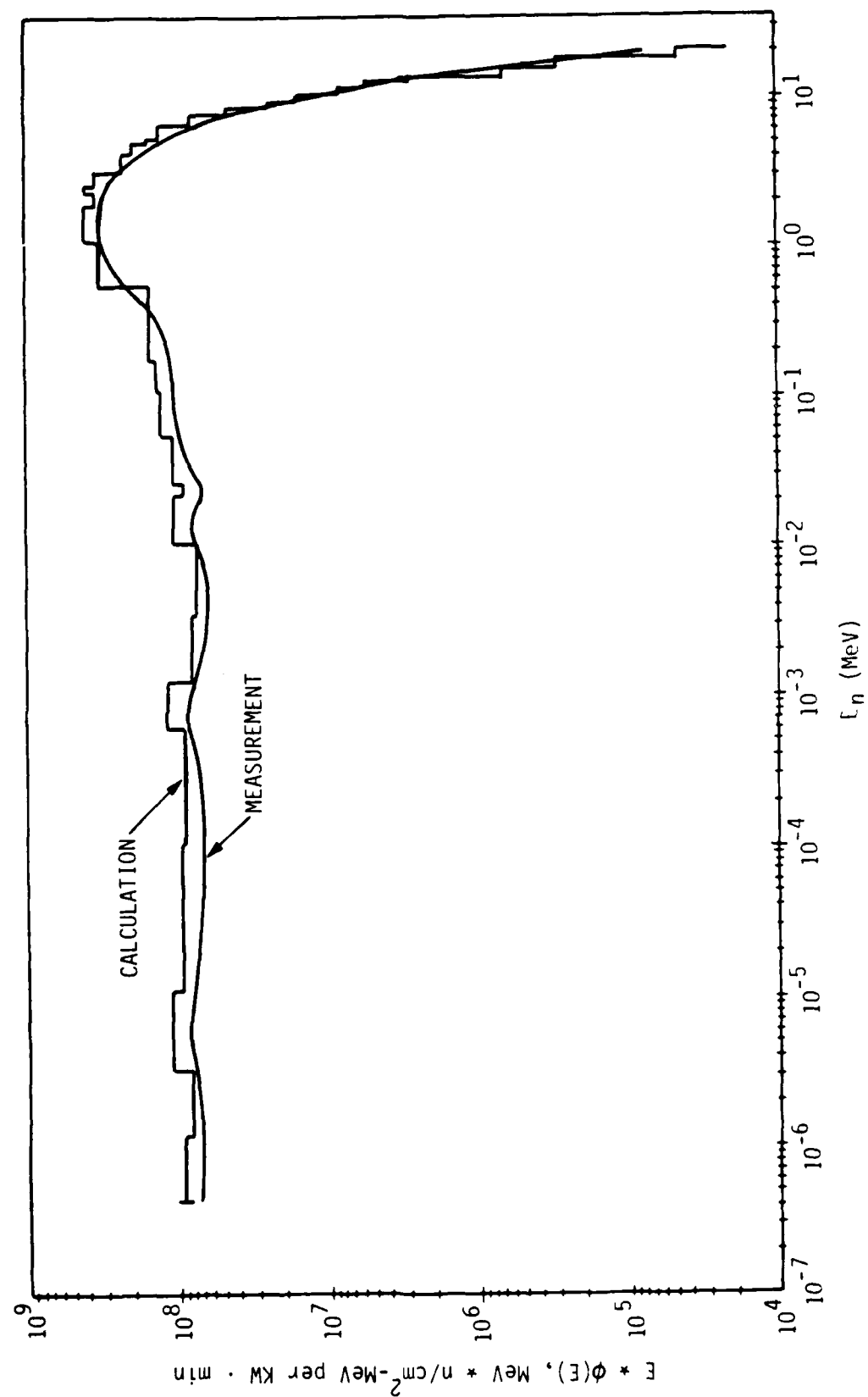


Figure 5. ERL, Mid-Thorax, Max, Absolute Comparison of Calculation with Baseline Measurement.

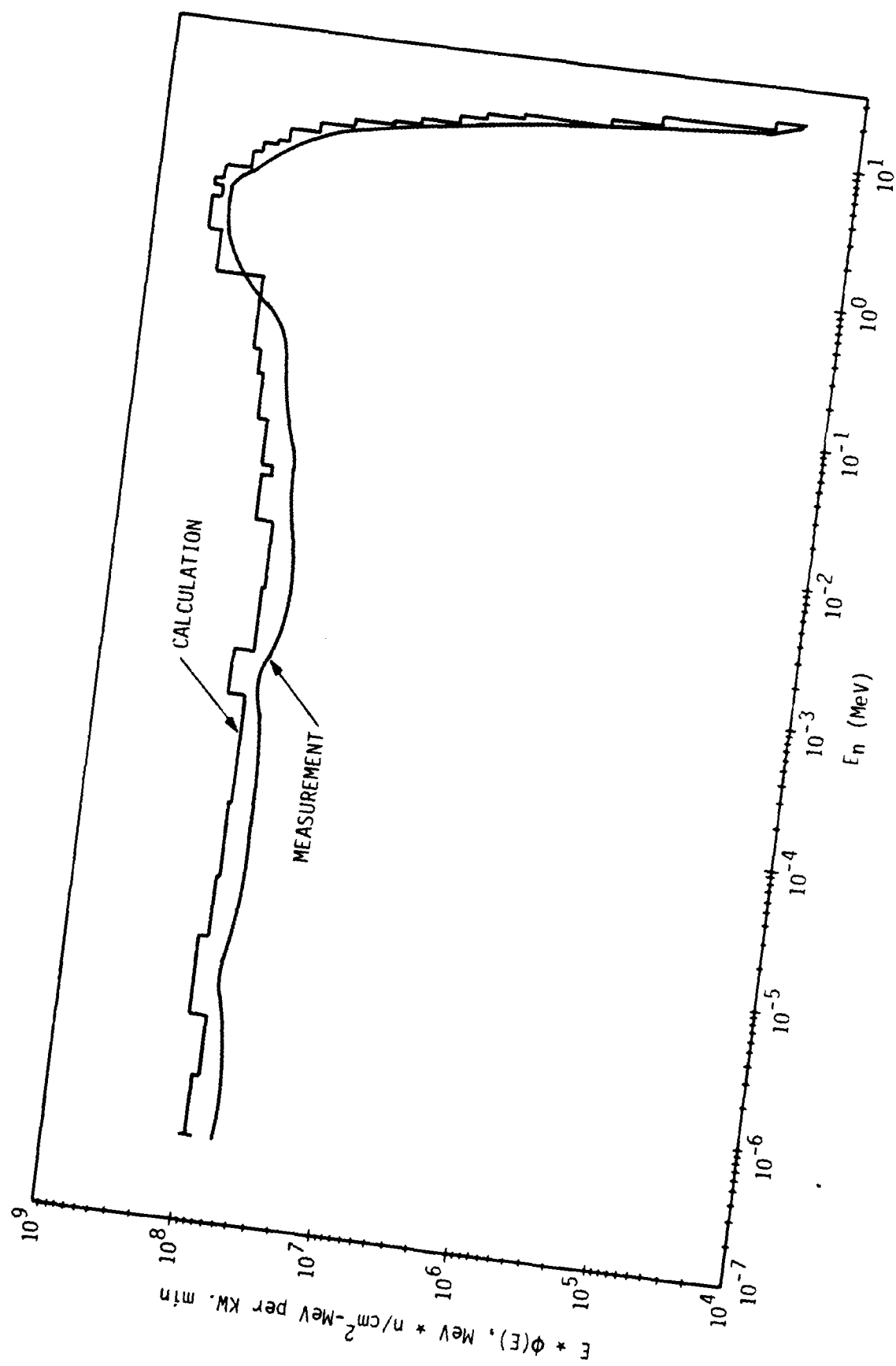


Figure 6. ER1 Mid-Thorax. Min. Absolute Comparison.

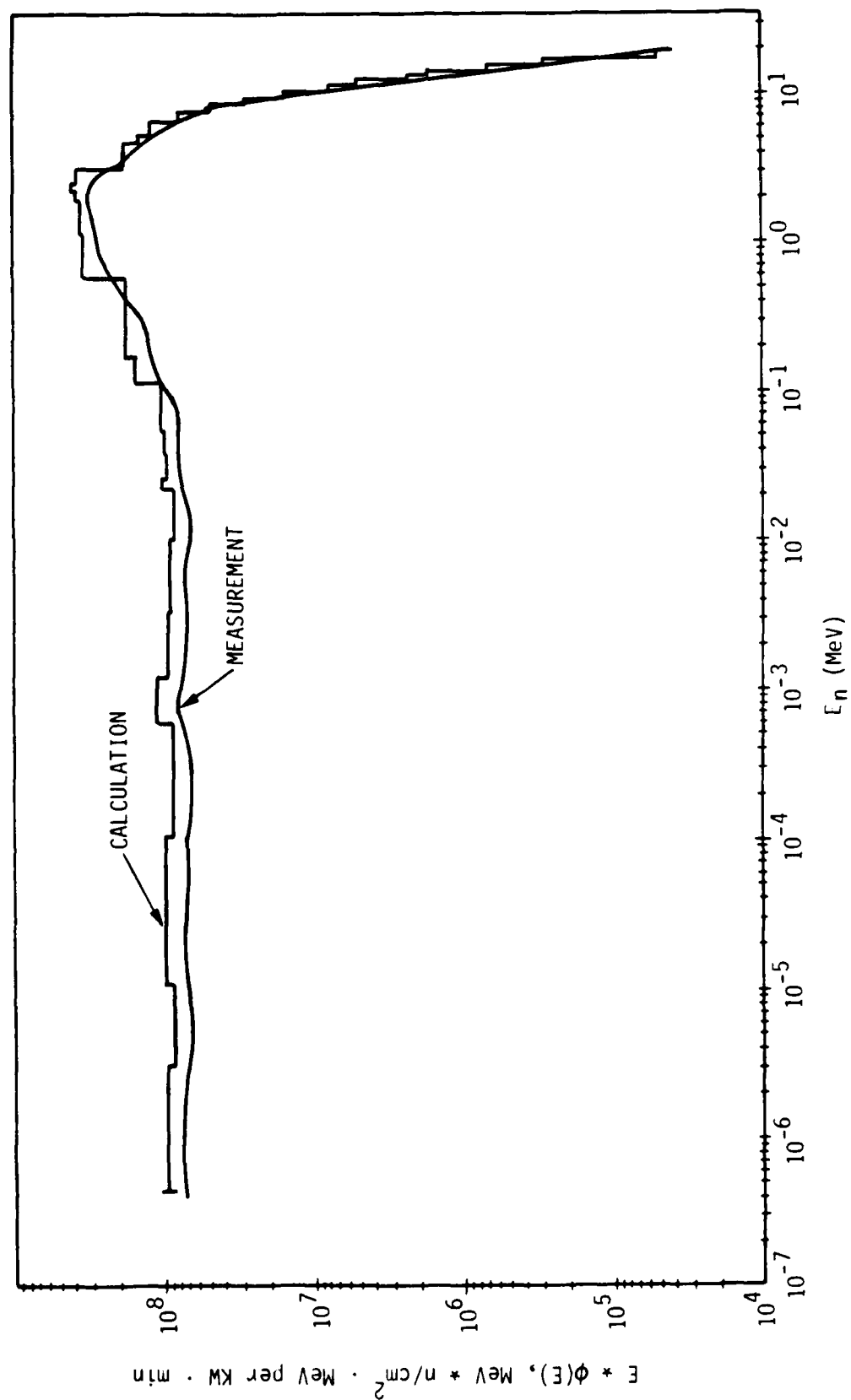


Figure 7. ERL, Head, Absolute Data.

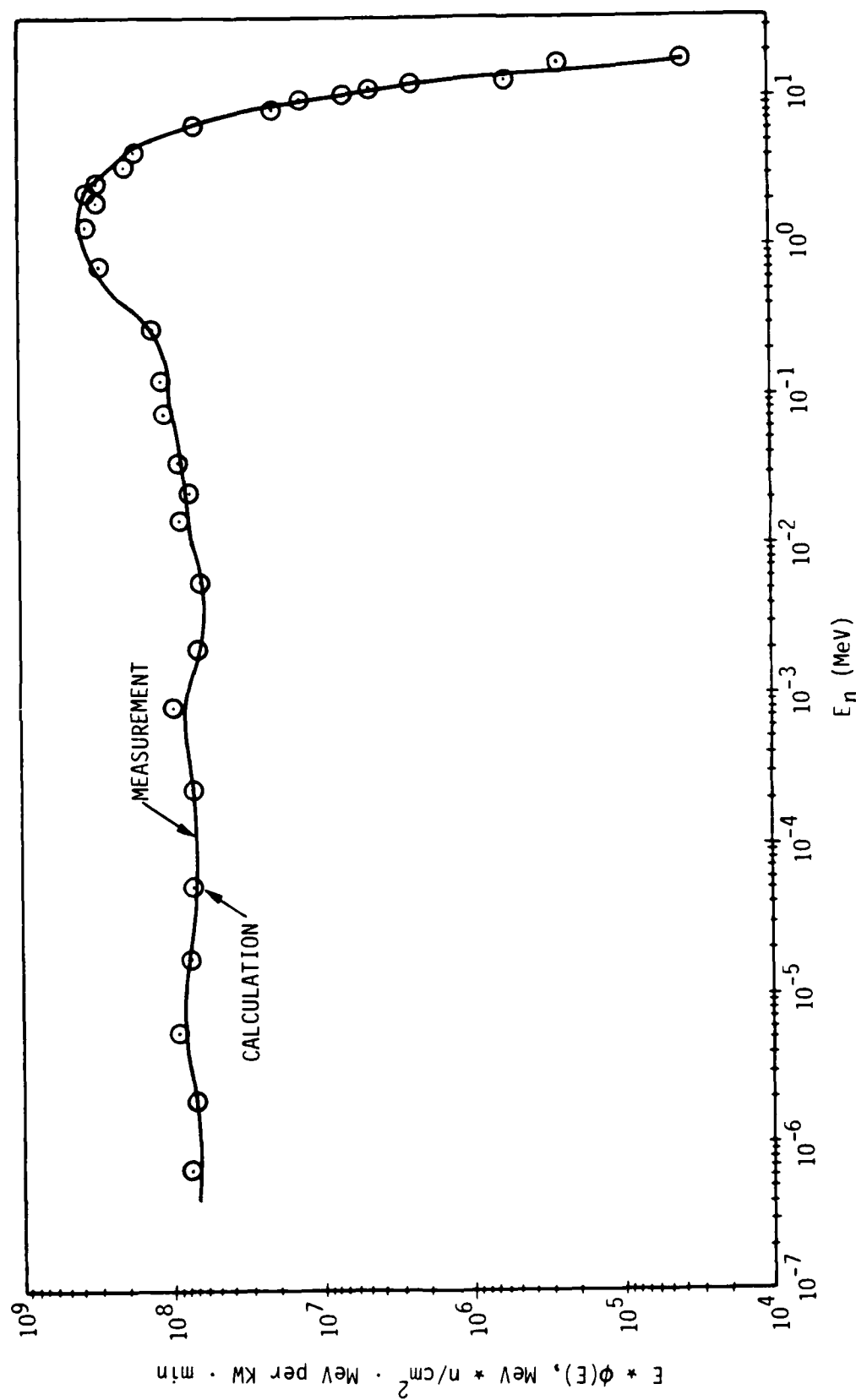


Figure 8. ERL-Hip, Measured, with Calculated Trail-Spectrum (Mid-Thorax) Filtted to it.

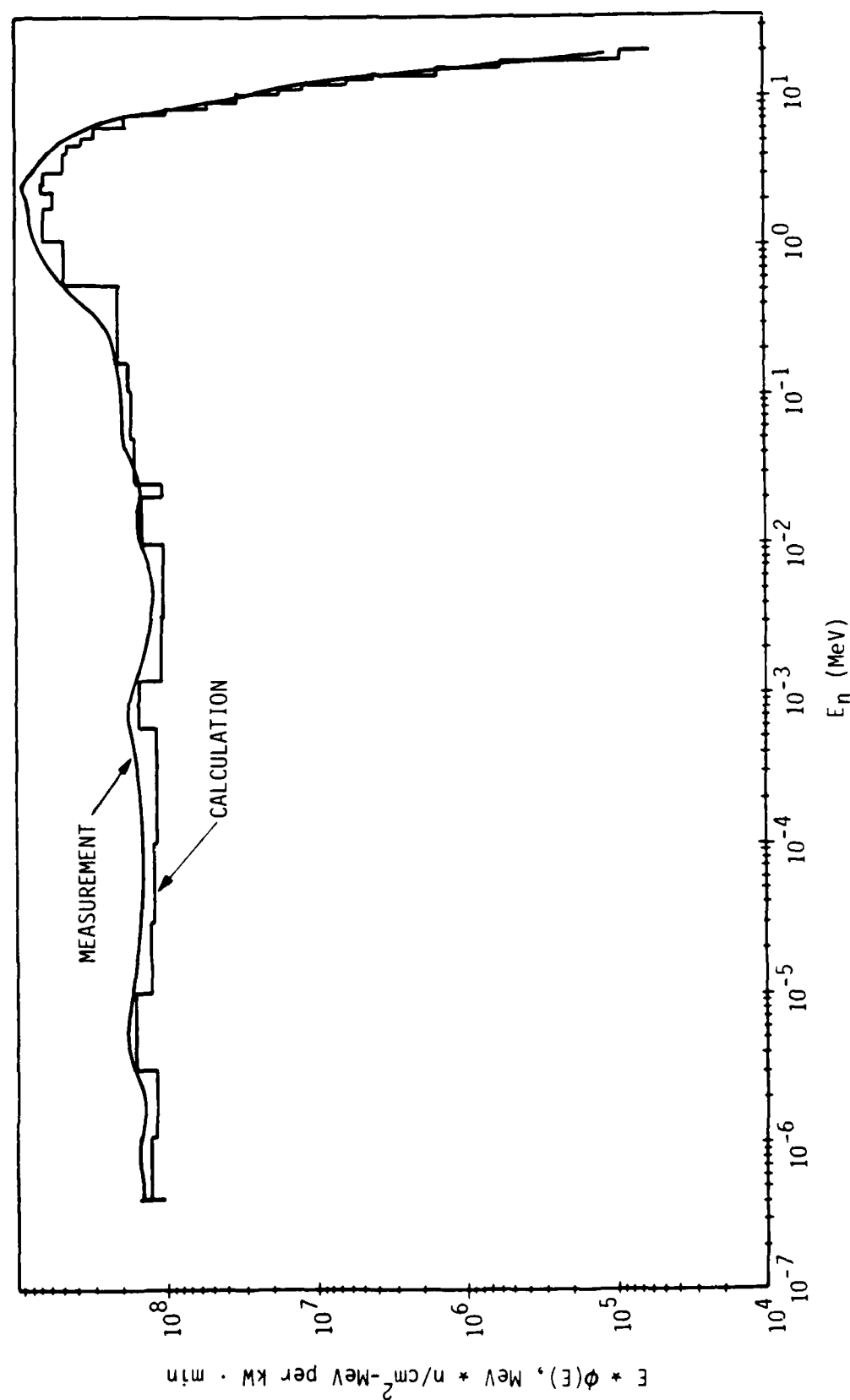


Figure 9. ER2, Mid Thorax, Absolute Fluences.

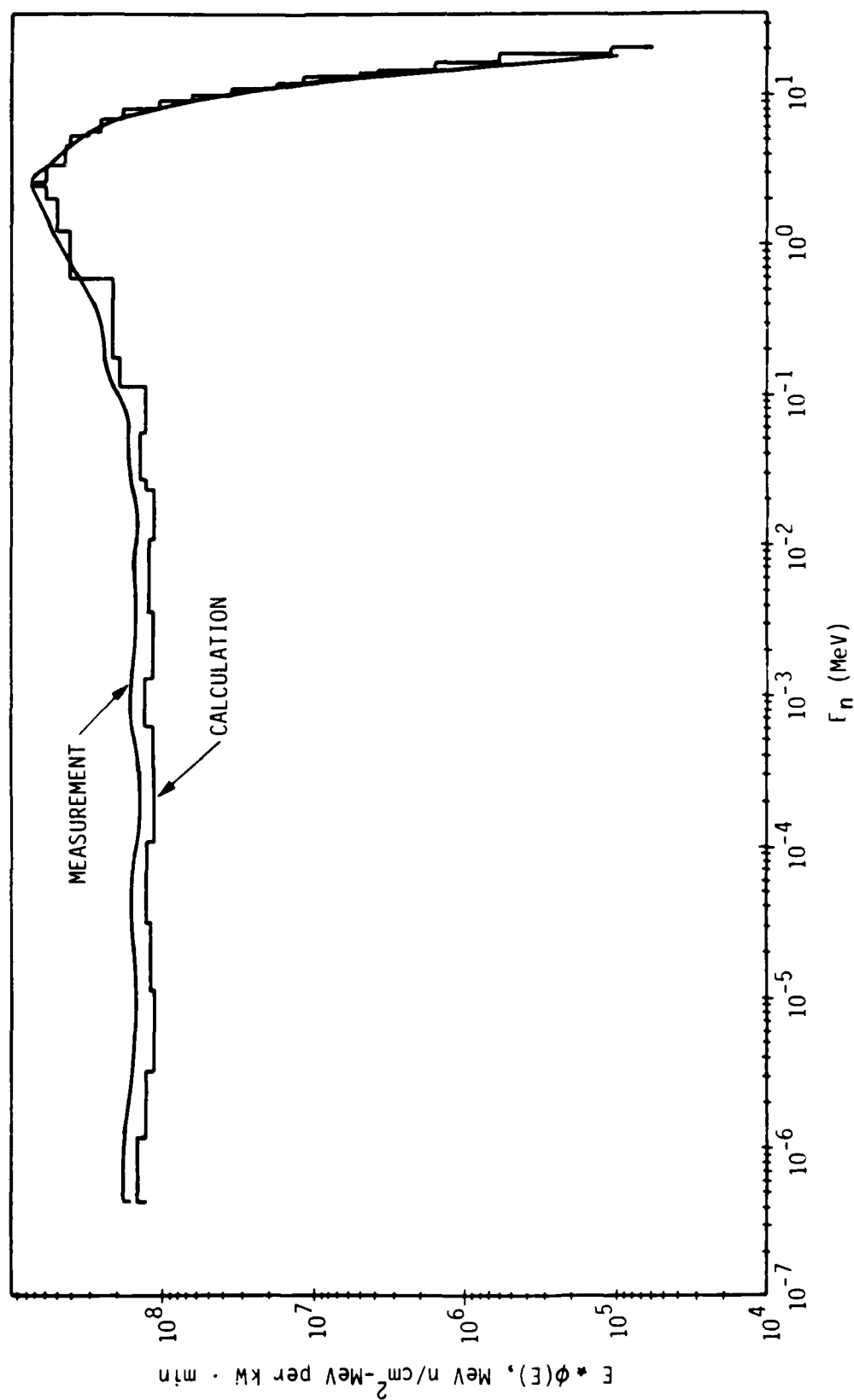


Figure 10. ER2, Head, Absolute Data.

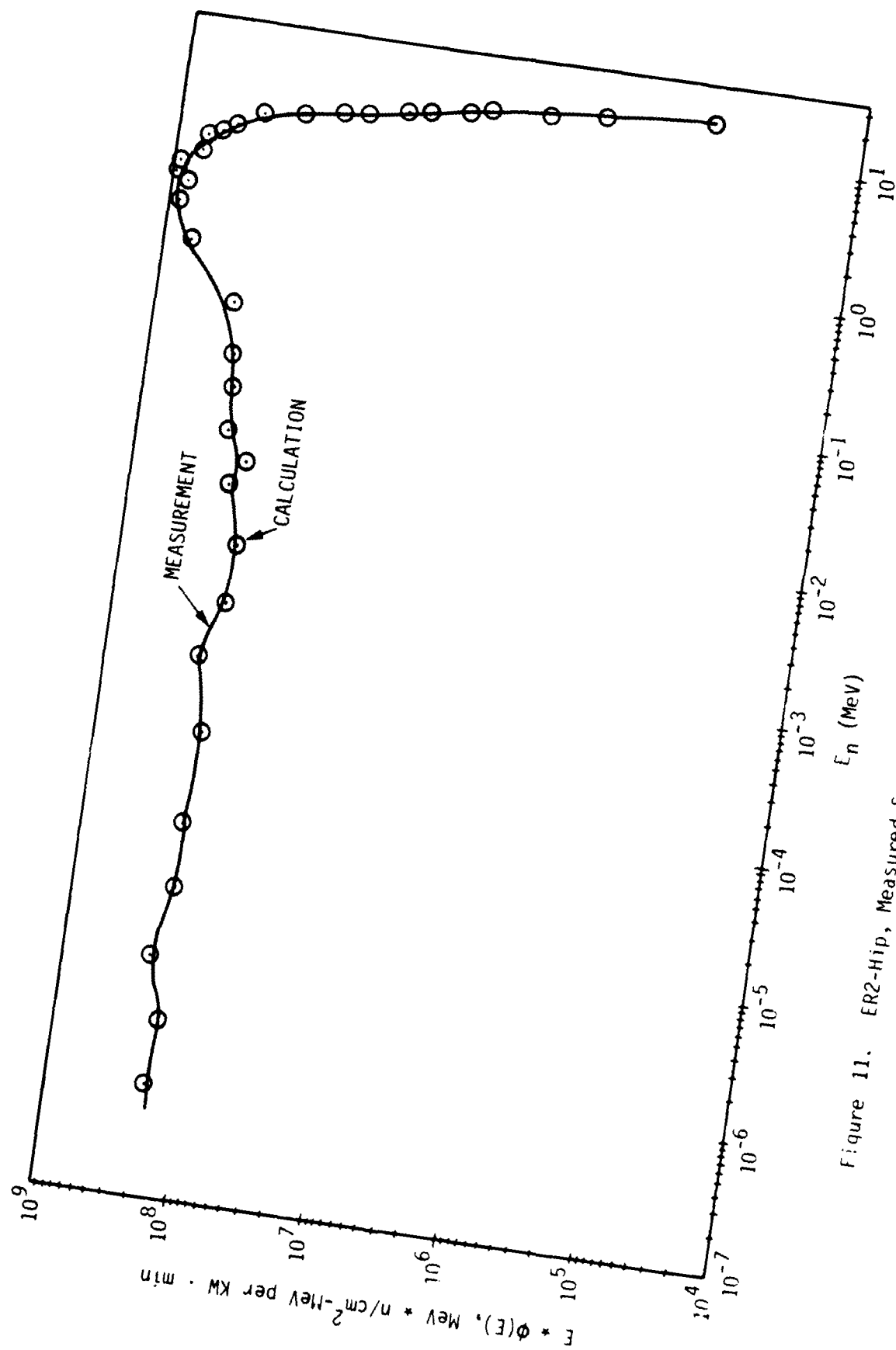


Figure 11. ER2-Hip, Measured Spectrum with Trial Spectrum Normalized to it for Shape Comparison.

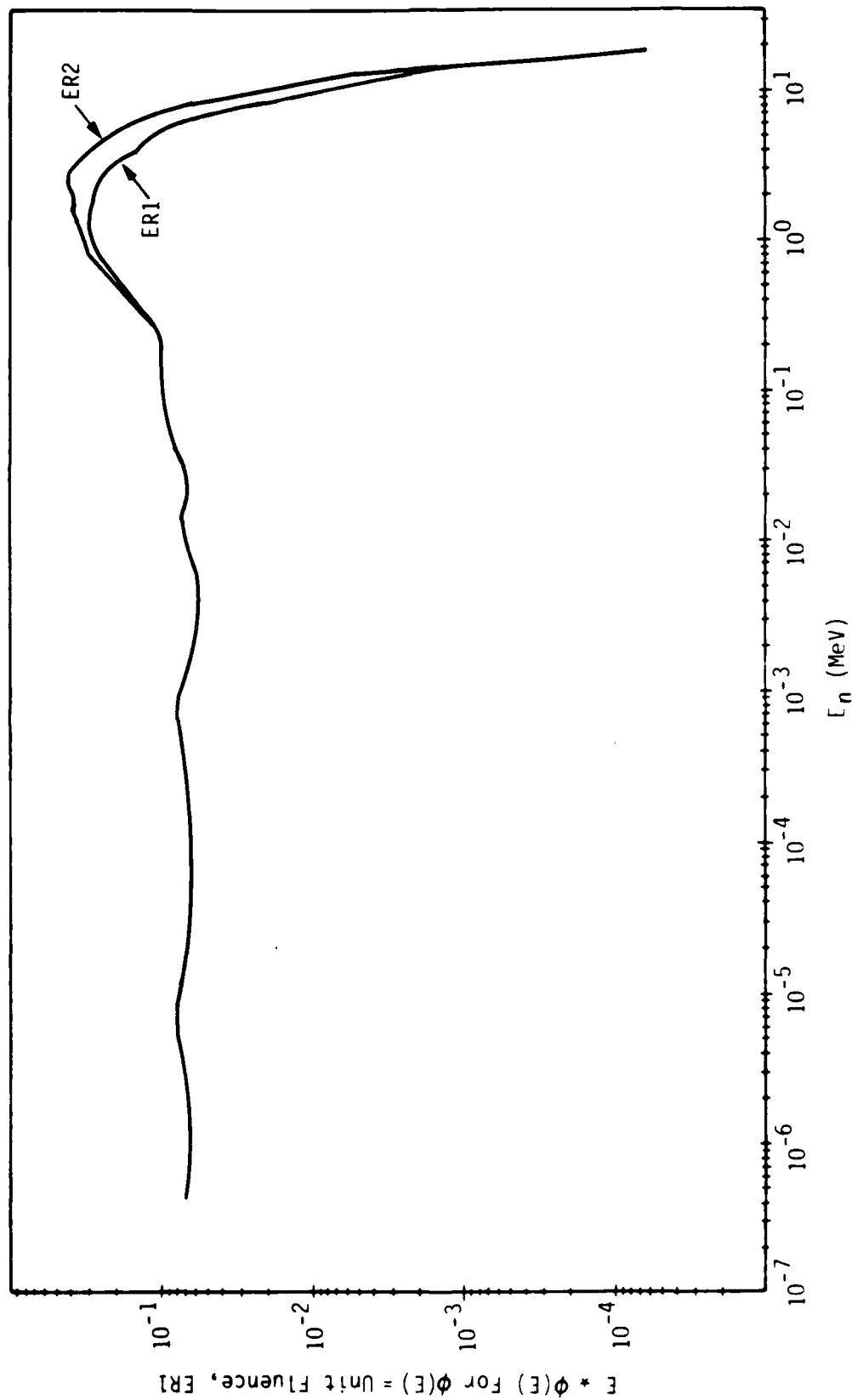


Figure 12. Spectrum-Shape Comparison, Mid Thorax: Effects of Lead-Wall Shield (ER1).

to be appreciably softer due to the lead wall. Inelastic scattering in the lead shield depletes this high-energy region from 0.4 MeV on up.

3.2 COMPARISONS OF AFRRRI ZOOLOGICAL PHANTOM MEASUREMENTS WITH CALCULATIONS NORMALIZED TO NICKEL FOIL MONITORS .

Neutron fluences have been measured and calculated for mid-head and mid-thorax locations in a simple zoological phantom exposed at the AFRRRI TRIGA reactor facility. The calculated data have been produced by Kaul et al,⁶ per unit free field KERMA and were first normalized to free field KERMA measured at the intended experiment location, 100 cm from the reactor centerline as follows:

Exposure Room 1 with 2" lead wall
7.8 Rad(tis) per Kw-Min

Exposure Room 2 free field
10.8 Rad(tis) per Kw-Min

The experimental measurements in ER1 were performed at 130 cm from the core centerline rather than 100 cm. Thus, the reported calculations had consequently been adjusted by Verbinski-Cassapakis by dividing by 1.617, a factor determined from measurements made at similar reactors. The calculational results were substantially greater than the measurements, differing by factors ranging from 20 to 100%, which brought to question the practice of normalizing the calculations to standard neutron dosimeters and comparing the results to the much more sophisticated dosimetry measurements presented here.

Because these calculation-measurement discrepancies are much larger than those reported in a similar comparison reported by Kaul et al, it was decided to reexamine the measurement-calculation comparison based on a normalization to nickel foil activation (Ni-58 (n,p) Co-58) data taken at the same time as the phantom measurements. The nickel foils were taped to the aluminum "dimple" which protrudes into each exposure room and into which the reactor is moved at the time of each experiment (see Figure 2). They were positioned at the

reactor midplane along a direct line to the phantom. The nickel foil results, in terms of disintegrations per second per Kw-Min per Ni-58 atom, at exposure time, are as follows:

$$\frac{ER1(W/Lead)}{5.33 \times 10^{-22}}$$

$$\frac{ER2(W/O Lead)}{6.11 \times 10^{-22}}$$

These values are converted to atoms of Co-58 per Kw-Min per atom of Ni-58 based on a Co-58 disintegration rate of 1.125×10^{-7} per sec., as follows:

$$4.74 \times 10^{-15}$$

$$5.43 \times 10^{-15}$$

The free field fluences on which the phantom calculations are based have been performed using ANISN,⁷ a one-dimensional discrete ordinates code, in a spherical geometry model which includes the reactor and all intervening detail. The calculated neutron scalar fluences at the nickel foil locations have been used together with Vitamin-E/ENDF/B-V activation cross sections⁸ to calculate the numbers of Co-58 nuclei per Ni-58 nucleus per source neutron which are as follows:

$$1.76 \times 10^{-30}$$

$$1.50 \times 10^{-30}$$

Thus, the numbers of source neutrons per Kw-min required to calculationaly reproduce the measured activation in each room are:

$$2.69 \times 10^{15}$$

$$3.62 \times 10^{15}$$

Using these values, the neutron KERMA in units of Rad(tis) per Kw-Min at 100 cm from the reactor calculated using one-dimensional methods are:

$$6.13$$

$$9.27$$

which are, respectively, 78.6% and 85.8% of the AFRRRI monitor values taken at the same locations but on a different day.

The nickel foil-based source normalizations were used to obtain new phantom fluences for comparison with the experimental values. The renormalized calculational results and the experimental results are presented in Table 7. The agreement at the mid-thorax location for neutron energies greater than 10 KeV is 10% or better. Because the mid-head location is actually out of the reactor mid-plane it is expected that the calculated values will show an increase relative to those of the measurements (unless the calculations are corrected for the larger distance of mid-head to reactor center). This is the case for Exposure Room 2 in the bare configuration. However, it is not the case in Room 1, which has the lead shield. The lead appears to have the effect of creating a more uniform exposure over the phantom. For energies below 10 KeV the agreement between calculation and experiment is no better than 10% and is generally much worse. This is most likely the result of using an overly simplified exposure field model.

3.2.1 Summary .

Good agreement has been obtained between calculated and measured fast fluence and KERMA values inside a zoological phantom exposed at the AFRR1 TRIGA reactor. This agreement has been obtained on the basis of normalization to nickel activation foil monitor data taken on the face of the reactor containment. Earlier comparisons in which calculations were normalized to paired chamber monitor data taken at the nominal experiment location yielded much poorer agreement. It is expected that better agreement can be obtained at low neutron energies and at locations out of the reactor midplane by using free field fluences obtained by two-dimensional methods, as contrasted to the one-dimensional calculations presented here.

Table 7. Four-Group Comparison of Calculated Neutron Fluence and Dose with Baseline Measurements
Values per Kw-min at 130 cm (ER1) and 100 cm (ER2) from Reactor Centerline.

Upper Energy (MeV)	ER1 (2" Lead Wall)				ER2 (Free Field)			
	Mid-Thorax		Mid-Head		Mid-Thorax		Mid-Head	
	n/cm ²	Rad(t/s)	n/cm ²	Rad(t/s)	n/cm ²	Rad(t/s)	n/cm ²	Rad(t/s)
1.96+1	Calc.	4.09+8	1.38+0	3.95+8	1.31+9	4.56+0	1.24+9	4.34+0
	Meas. c/m	4.53+8 .90	1.53+0 .90	4.26+8 .93	1.29+9 1.02	4.51+0 1.01	1.06+9 1.17	3.70+0 1.17
1.11+0	Calc.	5.71+8	6.54-1	5.78+8	1.39+9	11.61+0	1.32+9	1.56+0
	Meas. c/m	5.55+8 1.03	6.77-1 .97	5.70+8 1.01	1.27+9 1.09	1.54+0 1.05	1.24+9 1.06	1.41+0 1.11
1.03-2	Calc.	7.57+8	7.60-3	7.67+8	1.82+9	1.82-2	1.77+9	2.04-2
	Meas. c/m	6.30+8 1.20	6.73-3 1.13	7.47+8 1.03	1.48+9 1.23	1.56-2 1.17	1.63+9 1.09	1.89-2 1.08
4.14-7 (Thermal)	Calc.	3.35+9	7.49-2	2.59+9	1.05+10	2.36-1	8.52+9	1.91-1
	Meas. c/m	2.84+9 1.18	6.37-2 1.18	2.96+9 0.88	1.20+10 0.88	2.68-1 0.88	8.86+9 0.96	1.97-1 0.96
All	Calc.	5.09+9	2.12+0	4.33+9	1.50+10	6.42+0	1.29+10	6.11+0
	Meas. c/m	4.48+9 1.14	2.28+0 0.93	4.70+9 0.92	1.60+10 0.94	6.33+0 1.01	1.28+10 1.01	5.33+0 1.15

*Normalized to Nickel Foil monitors on containment face.

SECTION 4

THE 5-FOIL NEUTRON DOSIMETRY METHOD

This section presents a simple hand-calculational (perturbation) method of threshold-foil dosimetry in which 5 threshold-activation foils are used. (The SAND II code is not required; neither is there need for a trial spectrum. However, the "incremental doses" assigned to each foil (Table 8) were derived from the SAND II basepoint measurement.) One foil, the nickel foil, is used to derive the first-order dosimetry value, $D^0(\text{Ni})$. This is simply equal to D^B , the dose of the baseline run (i.e., the "standard" run in Table 4), multiplied by the ratio of the nickel-foil activations.

$$D^0(\text{Ni}) = D^B R(\text{Ni}) \quad 4.1$$

where $R(\text{Ni}) = (N_0 \lambda)^X(\text{Ni}) / (N_0 \lambda)^B(\text{Ni})$.

Here, $(N_0 \lambda)^X$ refers to the dosimetry measurement under consideration and $(N_0 \lambda)^B$ refers to the baseline-run value (the value for mid-thorax, ER1, in Table 3).

Now, if there were no change of spectral shape between the baseline run and run x, Equation 4.1 would give an accurate measure of the dose: The nickel foil has proven to be, by far, the most reliable foil in terms of reproducible results.

The nickel foil by itself cannot, of course, correct for a change of spectral shape. However, the foils with thresholds at energies different from the nickel threshold of about 3 MeV do provide change-of-spectral-shape data. This is done by means of the following "shape-perturbation" correction.

$$D^X = D^0(\text{Ni}) * \sum_i (A_i F_i - 1) \quad 4.2$$

Here, the A_i refers to the activation ratios of the i -th foil (i.e., Au, In, Fe and Mg) for the unknown and the baseline run, divided by $R(\text{Ni})$: i.e.,

$$A(\text{Au}) = R(\text{Au})/R(\text{Ni})$$

where

$$R(\text{Au}) = (N_0 \lambda)^X(\text{Au}) / (N_0 \lambda)^B(\text{Au}).$$

The various F_i refer to the fraction of the dose "sensed" by the i -th foil, in the case of the baseline run, excluding the nickel foil. The F_i values were determined from the dose values $D_{\text{STD}}(R)$ given in Table 8 for the "standard" or baseline run; i.e., the ER1, mid-thorax, full-stack spectrum. The corresponding energy range (region of maximum influence) for each foil is also presented in Table 8. Table 9 presents the value of F_i for each of the 4 "shaping-sensing" foils.

4.1 APPLICATION OF THE SIMPLE 5-FOIL DOSIMETRY METHOD.

The foil-activation values presented in Table 3, for all six (6) spectrum measurements, were utilized to provide the doses in phantom by means of Equations 4.1 and 4.2 above. The dose-fractions F_i , Equation 4.2, are given in Table 9 for each "shape-correction" foil i (i.e., Au, In, Fe and Mg).

The values of A_i (i.e., $R(\text{Mg})/R(\text{Ni})$) are presented in Table 9, along with $D^0(\text{Ni})$, the first order nickel-foil dose determination, and D^X , the second order determination in which a change-of-spectral-shape correction has been applied. Note how the A_i systematically increase with neutron energy for the ER2 spectra: As shown in Figure 11, these spectra are appreciably harder than the ER1 spectra, due to the down-scattering (in energy) of neutrons by the 2-inch thick lead wall in ER1.

The values of D^X are presented in Table 9, along with D^S , the values derived from the SAND II unfolding-code spectra. The last row presents the percent variation of D^X from D^S . The standard deviation for the ER1 (excluding mid-thorax) and ER2 data are 6%.

Table 8. Standard Run* Parameters for Short-Stack Dosimetry at AFRR1 .

Foil	Represented Energy Range		$(N_0 \lambda)_{STD} (\text{sec}^{-1})$	N^+_{STD}	$D_{STD}(R)^{++}$
	$E_L (\text{MeV})$	$E_U (\text{MeV})$			
^{197}Au	4.14-7	0.55	6.68-16	2.09+4	1460.2
^{115}In	0.55	2.31	2.25-17	7.03+2	4551.4
^{54}Fe	2.31	3.01	5.87-21	1.83-1	1114.6
^{58}Ni	3.01	6.38	3.20-20	1	2142.9
^{24}Mg	6.38	19.6	6.08-20	1.90+0	375.4

* The phantom mid-thorax exposure behind 2" lead at ER1 is taken to be the standard run.

N^+_{STD} is the Ni-normalized foil activation.

$^{++} D_{STD}(R)$ are doses for the 4187.5 kW · Min exposure, between E_L and E_U . Columns 2 and 3, taken from the basepoint ("standard") measurement, Table 4, but with ICRP rather than ICRU dose conversions. The ICRP vs. ICRU differences are irrelevant here.

Table 9. Dose Determinations via 5-Foil Dosimetry Stack for Epithermal Neutrons, per kW · Min.
 Compared to D_5 from SAND II Unfolding with 5 Folds. Doses in Rad (Tissue) per kW · Min.
 The D^0 and D^H Values are Hand-Calculated Values (See Equations 4.1 and 4.2).

	F_1	ERI (2" Lead)			ER2 (No Lead)		
		Mid-Thorax	Head	Hip	Mid-Thorax	Head	Hip
D^S (Epithermal)		2.22	2.15	2.81	6.06	5.13	7.21
R(Au)/R(Ni)	0.20	1.00	0.970	0.954	0.746	0.780	0.778
R(In)/R(Ni)	0.60	1.00	0.986	1.067	0.867	0.900	0.917
R(Fe)/R(Ni)	0.15	1.00	1.027	1.041	0.993	0.991	0.953
R(Mg)/R(Ni)	0.05	1.00	1.011	0.941	1.075	1.047	1.074
R(Ni)		1.000	0.98	1.19	3.38	3.75	3.72
D^0 (Ni)		2.22	2.10	2.64	7.49	6.11	8.26
D^H		2.22	2.08	2.60	6.53	5.48	7.45
$\Delta(S)(D^H-D^S)$		---	-3.4	-8.0	+7.7	+6.8	+3.4

The 5-foil stacks for the mid-thorax spectrum, ER1, were taken from the baseline-run data presented in Table 2. When the SAND II code was run with the 5-foil stack, the resulting epi-thermal neutron dose was about 1% higher. This is somewhat representative of the error resulting from utilizing a small fraction of the full-foil-stack data. This is to be compared with the 6% standard deviation resulting from utilizing the same five foils, but without SAND II.

SECTION 5
COMPARISON OF SAND II (5-FOIL STACK) AND THE
SIMPLE 5-FOIL DOSIMETRY METHOD PRESENTED IN SECTION 4

The improvement, due to the use of SAND II, derives from making full use of the a priori knowledge of the spectral shape. This a priori knowledge is input to SAND II in the form of the trial spectrum; i.e., the spectrum from the best available calculation. Thus, SAND II also represents a perturbation method of neutron spectrometry/dosimetry. The best-known (input) spectrum is perturbed in shape and absolutely adjusted in magnitude to agree with the foil-activation data.

The 5-foil dosimetry method presented in Section 4 can be thought of as a perturbation method as well in that it corrects for variations in spectral shape via an approximate 5-group ("histogram") approach. By contrast, SAND II makes full utilization of the a priori knowledge of the spectral shape. However, the estimated 6% accuracy for the 5-foil 5-group "histogram" method may be adequately accurate, compared to the 3-4% estimated accuracy for the maxi-foil dosimetry stack used with SAND II. Consider further that no accurate a priori knowledge of spectral shape is needed for the 5-foil 5-group "histogram" method of Section 4, making it much easier to apply.

The estimated 6% accuracy is to be contrasted to the inaccuracies implied in Section 3.2, where the calculational results⁶ were first obtained via normalization to measured free field KERMA (measured with TE dosimeters). Discrepancies ranging from 20 to 100% were reduced to the order of 10%, according to Section 3.2. This section, as well as Section 3.2.1, was taken directly from a communication by Dean Kaul (Letter, August 22, 1985).

SECTION 6

THERMAL (SUB-CADMIUM) NEUTRON DOSE

The thermal-neutron dose is derived from gold foil data, utilizing the cadmium-difference method. The gold-foil cross section is taken as 78.54 barns, which is the cross section derived from a Maxwellian thermal-neutron peak plus 1/E tail extending out to 0.414 eV. This cross section value is more accurate than the value of 98.8 barns, for 2200 m/sec neutrons.

A value of 2.24×10^{-11} rads per unit neutron fluence is the proper dose conversion factor (ICRU muscle KERMA).

It must be pointed out that the bare and cadmium-covered gold (or manganese or cobalt) foils cannot be exposed one behind the other, or even side-by-side, because of the cadmium-produced local flux depression: If side-by-side, but well separated (say by 3 or 4 cadmium "diameters"), then it is incumbent on the experimenter to prove that both are in identical epicadmium neutron-flux fields. In the measurements presented here, the bare foils were exposed in separate reactor runs, with run-to-run normalization carried out with nickel activation foils taped to the reactor entrance window (on the front of the "dimple" in Figure 2).

These nickel monitor foils proved to be a fortunate choice because they provided a basepoint for the "reactor power" or "reactor source term" renormalization. This is an otherwise formidable task, requiring flux plots throughout the reactor, an exact knowledge of day-to-day secondary standard (fission chamber, say) calibration, of the thickness of water between reactor and exit window to ER1/ER2, etc. (Prior to this, the calculation was renormalized to some dosimeters used at a much different time. This proved unfortunate, as can be seen from the results of Table 4, for example. Renormalization to the nickel foils on the dimple provided a meaningful comparison of measurement and calculation, which would have otherwise proven untenable.)

SECTION 7

LIST OF REFERENCES

1. V.V. Verbinski, et al, "Threshold-Foil Measurements of Reactor Spectra for Radiation Damage Applications," Nuclear Science and Engineering 65, 316 (1978).
2. V.V. Verbinski, et al, "Transistor Damage Characterization by Neutron Displacement Cross Section in Silicon: Experimental," Nuclear Science and Engineering 70, 66 (1979).
3. V.V. Verbinski, "Simultaneous Neutron Spectrum and Transistor-Damage Measurements in Diverse Neutron Fields: Validity of $D_{Si}(E_n)$," NRL Memorandum Report 3929, Naval Research Laboratory, March 16, 1979.
4. ASTM Standards Derived from References 1-3; E 720-80, E 721-80, E 722-80 and E 763-80.
5. V.V. Verbinski, et al, "Radiation Field Characterization for the AFRRI TRIGA Reactor," DNA 5793F-1, Defense Nuclear Agency, 1 June, 1981.
6. Kaul, D.C., et al, "Phantom Dosimetry Calculations for Use in Radiation Effect Correlations," DNA-TR-83-51, Defense Nuclear Agency, 30 July, 1984.
7. Engle, W.W., Jr., "A User's Manual for ANISN," K-1693 (RSIC-CCC-254) Union Carbide Corporation, 30 March, 1967, rev. 6 June, 1973.
8. Weisbin, C.R., et al, "Vitamin-E: An ENDF/B-V Multigroup Cross-Section Library for LMFBR Core and Shield, LWR Shield, Dosimetry and Fusion Blanket Technology.

DISTRIBUTION LIST

DEPARTMENT OF DEFENSE

ARMED FORCES RADIOBIOLOGY RSCH INST
10CYS ATTN: MRCO MAJ LUCKETT

ASSISTANT SECRETARY OF DEFENSE
HEALTH AFFAIRS
ATTN: INTERNATIONAL ACTIVITIES

ASSISTANT TO THE SECRETARY OF DEFENSE
ATTN: ROOM 3E 1074

DEFENSE INTELLIGENCE AGENCY
ATTN: RTS-2B

DEFENSE NUCLEAR AGENCY
4 CYS ATTN: TITL

DEFENSE TECHNICAL INFORMATION CENTER
12CYS ATTN: DD

DEPUTY UNDER SECRETARY OF DEFENSE
ATTN: ENV & LIFE SCIENCES

FIELD COMMAND DEFENSE NUCLEAR AGENCY
ATTN: FCP/FCPF

INTERSERVICE NUCLEAR WEAPONS SCHOOL
ATTN: RH

DEPARTMENT OF THE ARMY

ARMED FORCES INSTITUTE OF PATHOLOGY
ATTN: RADIOLOGIC PATHOLOGY DEPT

DIRECTORATE OF COMBAT DEVELOPMENT
ATTN: ATSA-COM-L(NBC)

LETTERMAN ARMY INSTITUTE OF RESEARCH
ATTN: SGRD-ULV-R

SURGEON GENERAL
ATTN: AAFJML
ATTN: MEDDH-N

U S ARMY ACADEMY OF HEALTH SCIENCES
ATTN: HSHA-CDD

U S ARMY NATICK RSCH DEV & ENGRG CENTER
ATTN: STRNC-S

U S ARMY NUCLEAR & CHEMICAL AGENCY
ATTN: MONA-NU

WALTER REED ARMY INSTITUTE OF RESEARCH
ATTN: DIV OF EXPER THERAPEUTICS

DEPARTMENT OF THE NAVY

BUREAU OF MEDICINE & SURGERY
ATTN: CODE 71

NAVAL AEROSPACE MEDICAL INSTITUTE
ATTN: ANIMAL BEHAVIORAL SC BR

NAVAL AEROSPACE MEDICAL RESEARCH LAB
ATTN: COMMANDING OFFICER

NAVAL MEDICAL COMMAND
ATTN: MEDCOM-21

NAVAL MEDICAL RESEARCH & DEV. COMMAND
2 CYS ATTN: (CODE 40C), NMCNCR

OFFICE OF NAVAL RESEARCH
ATTN: CODE 441

RADIATION HEALTH OFFICER
ATTN: USS SIMON LAKE (AS 33)

DEPARTMENT OF THE AIR FORCE

BOLLING AFB
ATTN: AF/SGPT
ATTN: HQ USAF/SGES

U S AIR FORCE ACADEMY
ATTN: HQ USAFA/DFBL

U S AIR FORCE OCCUPATIONAL & ENV HEALTH LAB
ATTN: OEHL/RZI

USAF SCHOOL OF AEROSPACE MEDICINE
ATTN: AEROSPACE MEDICAL DIV (AFSC)
ATTN: CHIEF, RADIOBIOLOGY DIV (RA)
ATTN: USAFSAM/RZB

DEPARTMENT OF ENERGY

ARGONNE NATIONAL LABORATORY
ATTN: REPORT SECTION

BROOKHAVEN NATIONAL LABORATORY
ATTN: REPORTS SECTIONS
ATTN: RESEARCH LIBRARY

DEPARTMENT OF ENERGY
ATTN: DIR OHER-ER 70

LAWRENCE BERKELEY NATIONAL LAB
ATTN: LIBRARY

DNA-TR-87-10 (DL CONTINUED)

LAWRENCE LIVERMORE NATIONAL LAB
ATTN: TECH INFO DIV LIB L-3

LOS ALAMOS NATIONAL LABORATORY
ATTN: REPORT LIBRARY

LOVELACE BIOMEDICAL &
ATTN: DOCUMENT LIBRARY

OTHER GOVERNMENT

CENTRAL INTELLIGENCE AGENCY
ATTN: OFFICE OF MEDICAL SERV

DIVISION OF LIFE SCIENCES, OST
9CYS ATTN: DIVISION OF LIFE SCIENCES, OST

GPO-CONSIGNED BRANCH
17CYS ATTN: CONSIGNED STOCK

LIBRARY OF CONGRESS
ATTN: EXCHANGE AND GIFT DIV

NATIONAL LIBRARY OF MEDICINE, NIH
ATTN: OFC OF PUB & INQUIRIES

NUCLEAR REGULATORY COMMISSION
ATTN: LIBRARY

PROJ OFFICER FOR RADIOLOGICAL MODIFIERS
ATTN: NIH-NCI-DCT-CTEP-RDB-BTSG

U S GOVERNMENT PRINTING OFFICE
ATTN: RM A-150

U S PUBLIC HEALTH SERVICE
ATTN: DIV OF BIOLOGICAL EFFECTS

U S PUBLIC HEALTH SERVICE
ATTN: NORTHEASTERN RADIO HEALTH LAB

DEPARTMENT OF DEFENSE CONTRACTORS

KAMAN SCIENCES CORP
ATTN: DASAC

KAMAN TEMPO
ATTN: DASAC

PACIFIC SIERRA RES LAB
ATTN: H BRODE, SAGE CHAIRMAN

SCIENCE APPLICATIONS INTL CORP
2 CYS ATTN: C G CASSAPAKIS
2 CYS ATTN: V V VERBINSKI

FOREIGN

NBC DEFENSE RESEARCH AND DEVELOPMENT
ATTN: WWDBW AB(SCHUTZ)

SERIAL ACQUISITIONS (EXCHANGE)
ATTN: BRITISH LIBRARY

DIRECTORY OF OTHER

CALIFORNIA, UNIVERSITY OF DAVIS
ATTN: RADIOBIOLOGY LAB

OREGON STATE UNIVERSITY
ATTN: DEPT OBIOCHEM & BIOPHY

RADIOISOTOPE LABORATORY
ATTN: RADIOISOTOPE LAB

ROCHESTER UNIV MEDICAL CTR
ATTN: RBB LIBRARY

END

DATE

FILMED

5-88

DTIC